

**HDMX-L IS EXPRESSED FROM A FUNCTIONAL P53-RESPONSIVE PROMOTER IN THE FIRST INTRON OF THE *HDMX* GENE, AND PARTICIPATES IN AN AUTO-REGULATORY FEEDBACK LOOP TO CONTROL P53 ACTIVITY\***

Anna Phillips<sup>1</sup>, Amina Teunisse<sup>2</sup>, Suzanne Lam<sup>2</sup>, Kirsten Lodder<sup>2</sup>, Matthew Darley<sup>1</sup>, Muhammad Emaduddin<sup>1</sup>, Anja Wolf<sup>3</sup>, Julia Richter<sup>3</sup>, Job de Lange<sup>2</sup>, Matty Verlaan – de Vries<sup>2</sup>, Kristiaan Lenos<sup>2</sup>, Anja Böhnke<sup>3</sup>, Frank Bartel<sup>3</sup>, Jeremy P. Blaydes<sup>1</sup> and Aart G. Jochemsen<sup>2</sup>

From <sup>1</sup>Southampton Cancer Research UK Centre, University of Southampton School of Medicine, UK, <sup>2</sup>Leiden University Medical Center, Dept. Molecular Cell Biology, Leiden, The Netherlands and <sup>3</sup>Faculty of Medicine, University of Halle-Wittenberg, Germany

Address correspondence to: Jeremy P. Blaydes, Somers Cancer Research Building, MP824, Southampton General Hospital, Southampton, U.K. SO16 6YD. FAX +44 (0) 2380 795152; Email [j.p.blaydes@soton.ac.uk](mailto:j.p.blaydes@soton.ac.uk), and Aart G. Jochemsen, Leiden University Medical Center, Dept. Molecular Cell Biology, P.O. Box 9600, 2300 RC Leiden, The Netherlands. FAX +31 (0)71 5268170; Email: [a.g.jochemsen@lumc.nl](mailto:a.g.jochemsen@lumc.nl).

The p53 regulatory network is critically involved in preventing the initiation of cancer. In unstressed cells p53 is maintained at low levels and is largely inactive, mainly through the action of its two essential negative regulators, HDM2 and HDMX. p53 abundance and activity are upregulated in response to various stresses including DNA damage and oncogene activation. Active p53 initiates transcriptional and transcription-independent programs that result in cell cycle arrest, cellular senescence or apoptosis. p53 also activates transcription of *HDM2*, which initially leads to the degradation of HDMX, creating a positive feedback loop to obtain maximal activation of p53. Subsequently, when stress-induced post-translational modifications start to decline, HDM2 becomes effective in targeting p53 for degradation, thus attenuating the p53 response. To date, no clear function for HDMX in this critical attenuation phase has been demonstrated experimentally. Like *HDM2*, the *HDMX* gene contains a promoter (P2) in its first intron that is potentially inducible by p53. We show that p53 activation in response to a plethora of p53-activating agents induces the transcription of a novel *HDMX* mRNA transcript from the *HDMX-P2* promoter. This mRNA is more efficiently translated than that expressed from the constitutive *HDMX-P1* promoter, and it encodes a long form of HDMX protein, HDMX-L. Importantly, we demonstrate that HDMX-L cooperates with HDM2 to promote the ubiquitination of p53, and that p53-induced *HDMX* transcription from the P2 promoter can play a key role in the attenuation phase of

**the p53-response, to effectively diminish p53 abundance as cells recover from stress.**

The tumor suppressor protein p53 functions primarily as a stress-inducible transcriptional activator of genes that promote cell cycle arrest and apoptosis (1). Stress-induced p53 activation can form a rate-limiting barrier to tumorigenesis (2,3), and the manipulation of p53 function is key to the mechanism of action of many cancer chemotherapeutic strategies (4,5). In unstressed cells p53 is maintained at low levels and inactive, largely through the action of several p53-inducible negative feedback pathways, the most extensively studied of which involves the oncoproteins HDM2 and HDMX (also called MDM4) (Mdm2 and MdmX/Mdm4 in mouse) (6,7). Considerable research effort has been applied to understanding the mechanisms whereby these two proteins regulate p53 function. HDM2 and HDMX both contain an N-terminal pocket which binds to the primary transactivation domain of p53; they can, therefore, function independently of each other to repress p53-dependent transcription (8-10). HDM2 also forms both HDM2-HDM2 homodimers and HDM2-HDMX heterodimers. These function as E3 ubiquitin ligases for p53; mono-ubiquitination of p53 by HDM2 inhibits p53 activity by both inhibiting acetylation and promoting nuclear export, while poly-ubiquitination promotes proteasome-mediated p53 degradation and is largely responsible for the rapid turnover of p53 protein that occurs in proliferating cells (11). HDMX itself lacks E3-ligase activity, and does not readily homodimerize, however, because HDMX-HDM2 heterodimerize with higher affinity than do HDM2-HDM2 homodimers, HDMX can effectively function to promote cellular HDM2

E3-ubiquitin ligase activity when cellular HDM2 concentrations are limiting (12-14). Conversely, at higher HDMX concentration, monomeric HDMX can potentially inhibit p53 ubiquitination by competing with the dimeric proteins for p53 binding (15). Thus both the absolute and relative abundance of HDM2 and HDMX in cells are critical determinants of p53-dependent transcriptional activity, and hence cellular proliferation and survival.

Germ line genetic changes that cause relatively modest increases or decreases in *HDM2/mdm2* expression promote (16) and protect (17) from tumorigenesis, respectively. Furthermore, many separate studies have identified both *HDM2* and *HDMX* as being over-expressed in diverse tumors, through a variety of mechanisms including, but not limited to, gene amplification (18). The mechanisms regulating expression of *HDM2/mdm2* have now been quite extensively studied. The *HDM2/mdm2* gene is transcribed from two promoters, one (P1) 'constitutive' and the second (P2), which is located 5' to exon 2, and is inducible by both p53 and mitogens (19-21). The transcripts from these two promoters are translated into full length (p90) HDM2/Mdm2 and N-terminally truncated, p53-binding incompetent, HDM2/Mdm2 proteins. The mRNA transcript from the P2 promoter is approximately eight fold more efficiently translated into full length, p90, HDM2/Mdm2 than that from P1 (22-24). Following genotoxic stress such as ionizing radiation (IR), the abundance of both HDM2 and HDMX proteins initially decreases, due to an ATM- and HDM2 E3-ligase-dependent increase in their degradation, thus promoting activation of p53 (25-28). HDM2 levels subsequently increase rapidly, due to p53-dependent transcription from the *HDM2-P2* promoter, facilitating the attenuation of the p53-response. Stress-induced reduction in HDMX protein abundance is more sustained and *HDMX* transcription is not reported to be induced by p53. Indeed whilst the overall gene structure of *HDMX/mdmx* is very similar to that of *HDM2/Mdm2*, *HDMX/mdmx*, an equivalent of the p53-inducible P2 promoter 5' to a non-coding exon 2 has not been reported in the *HDMX/mdmx* genes (6).

HDMX abundance can affect the level of the p53-dependent cellular response to ionizing radiation, ribosomal stress as well as to a chemical inhibitor of the p53-HDM2 interaction (Nutlin-3), that is under development as a

promising novel cancer therapeutic (7,29,30). There is, therefore, a clear necessity for an understanding of the pathways that regulate HDMX protein levels and how they may regulate the cellular response to both established and experimental cancer therapies.

Specific forms of genotoxic stress such as ultraviolet radiation, doxorubicin and cisplatin can induce aberrant splicing of *HDMX* mRNA as well as promoting the degradation of the full length *HDMX* mRNA, together resulting in the loss of expression of the full length protein (31,32). These studies, as well our original report first describing *mdmx* (9) have shown that total *HDMX/mdmx* mRNA abundance does not generally increase in response to DNA damage-induced p53 activation. This, as well as the increased rates of HDM2-dependent degradation of HDMX protein that follows p53 activation, means that HDMX protein abundance does not increase in response to genotoxic p53-activating signals, and that *HDMX* had not been identified as a p53-inducible gene. However, it is noteworthy that, when the upregulation of p53-responsive genes are studied in, for example, mouse tissues in response to ionising radiation, total *mdm2* mRNA levels increase by a maximum of two fold, even in tissues such as spleen and thymus where upregulation of another p53-responsive gene, *p21<sup>WAF1</sup>* is ~10 and 50 fold, respectively (33). This is because in these tissues basal levels of the *mdm2-P1* transcripts are up to 10 fold higher than those derived from the P2 promoter, and the fold increase in *mdm2-P2* transcript levels in response to radiation are only sufficient to cause modest changes in total *mdm2* mRNA abundance (34). Mdm2 protein synthesis can increase substantially in response to radiation, due to the increased translation potential of the *mdm2-P2* transcript, and thus clearly the lack of substantial changes in total mRNA abundance in this situation is potentially deceptive. Despite the overall similarity in the structure of the *HDMX/mdmx* and *HDM2/mdm2* genes, this possibility of the existence of alternate transcripts with quantitatively different translational potential within the total pool of *HDMX* mRNA in cells has not, to date, been investigated.

A study which aimed to identify novel p53-responsive genes by global genomic profiling of chromatin fragments bound by p53 identified a p53-binding region within the first intron of *HDMX* (35), and very recently synthetic reporter

constructs containing this region have been shown to drive of the reporter gene in a p53-dependent manner (36), suggesting that *HDMX* is indeed a p53-regulated gene. In this manuscript we show that, like *HDM2*, the *HDMX* gene contains a p53-responsive promoter in its first intron that drives the expression of mRNA transcripts with quantitatively and qualitatively different translation potential, and which participate in an auto-regulatory feedback loop to control the abundance and activity of p53 in cancer cells.

### Experimental procedures

**Cell culture and reagents-** MCF-7, SAOS-2, SAOS-2/p53 Tet-On (37), NARF and 174-2 cells (*p53/mdm2* DKO MEFs) were cultured in Dulbecco's modified Eagle's medium (Invitrogen) supplemented with 10% fetal calf serum. Early passage p53<sup>+/+</sup> and p53<sup>-/-</sup> murine embryo fibroblasts (MEFs) were maintained in DMEM, supplemented with 15% fetal calf serum and 0.5 mM 2-mercapto-ethanol, and grown at 3% oxygen. H1299, the breast carcinoma cell lines MPE600 and ZR75-30, the uveal melanoma cell lines MEL285 and 92.1 (38), N-TERA-2, 833KE and mouse melanoma B16F10 cells were cultured in RPMI-1640 supplemented with 10 % fetal calf serum. The generation and culture conditions of MCF-10A (M1) and MCF-10AT (M2) cells has been described (39).

To generate stable p53 knockdown and control knockdown cell lines, cells were infected with lentiviral vectors expressing shRNA targeting human *p53* or mouse *mdmx*, and conferring puromycin resistance. The latter does not target the *HDMX* mRNA. After puromycin selection, polyclonal cell lines were established. Nutlin-3 (Alexis Biochemicals) was dissolved in ethanol at 5 mM, MG-132 (Sigma) in DMSO at 10 mM, before adding to the medium where stated. 5-fluorouracil (Sigma) was in aqueous solution. Etoposide (Sigma) was dissolved in DMSO at 10 mM, Leptomycin B (BIOMOL) in ethanol at 10  $\mu$ M, and Actinomycin D (Calbiochem) in ethanol at 1 mg/ml. Neocarzinostatin was obtained from Sigma.

**Protein analysis-** Cells were washed with phosphate-buffered saline, pelleted by centrifugation at 1000 x g, snap-frozen, and stored at  $-80^{\circ}\text{C}$ . Immunoblotting was performed as described previously (40), and

membranes were probed for HDMX (A300-287A, Bethyl Laboratories), HDM2 (monoclonal antibody 2A9 or 4B2 (41)), p53 (DO-1, Serotec), GFP (Cancer Research UK), PUMA (Cell Signaling Technology), p21<sup>WAF-1</sup> (EA10, Calbiochem or CP74, Millipore), KAP1 and Phospho-KAP1/P-S824 (A300-274A and A300767A), PARP (Cell Signaling Technology) and HAUSP (A300-033A, Bethyl Laboratories). Anti-phospho-H2AX was obtained from Millipore. Mouse Mdm2, Mdmx, p53 and HAUSP were detected with, respectively, mouse monoclonal 4B2, (41), MX-82 (Sigma), 1C12 (Cell Signaling) and mouse monoclonal 1G7 (42). Equal protein loading was confirmed on all immunoblots using rabbit anti  $\beta$ -actin or anti-tubulin antibodies (Sigma-Aldrich). Bands were visualized by chemiluminescence (Supersignal, Pierce) using a Fluor-S MAX system (Bio-Rad) or by exposure to X-ray films (Fuji). In the IP/Western analysis of HDMX:p53 interactions, the IPs were performed with either anti-HA rabbit polyclonal (Abcam) or anti-Flag rabbit polyclonal (Sigma), after which the blots were incubated with either anti-Flag monoclonal antibody M2 (Sigma) or anti-HA monoclonal antibody HA.11 (Covance). Detection of p14<sup>ARF</sup> by immunofluorescence was performed with anti-p14ARF monoclonal antibody 4C6 (gift of Gordon Peters).

**RNA analysis-** For RT-PCR analysis of transcripts, 0.5-2  $\mu$ g of RNA was reverse transcribed in a 20-25  $\mu$ l volume using Superscript II RNase H<sup>-</sup> reverse transcriptase (Invitrogen) and oligo(dT) primer. Two  $\mu$ l of cDNA product were used as target in 50  $\mu$ l of PCR reactions using GoTaq DNA polymerase (Promega). RT-PCR analysis of *HDM2-P2* and  *$\beta$ -actin* transcripts was as described previously (21). Primer sets used in the various RT-PCR experiments are presented in Supplementary Table 1.

**Plasmids-** Genomic *HDMX-P2* sequence was amplified from normal human liver DNA and ligated into pGL3-Basic using the MluI/XhoI sites (Promega) to generate reporter construct HDMXP2luc01. The sequence of the inserted 1332-bp region (-1535 to -202, relative to the start of exon 2) was identical to RefSeq NT\_004487. Additional constructs containing deletions of the *HDMX-P2* promoter (luc02-08) were generated using additional primers. 3-bp substitutions in the putative p53 binding site were introduced into HDMXP2luc01 to give HDMXP2luc01 $\Delta$ p53RE using the QuikChange

mutagenesis kit (Stratagene), and verified by sequencing. Expression vectors containing cDNA (including 5'UTR, coding sequence and a C-terminal mychis tag) for both HDMX-P1 and HDMX-P2 were created by ligation of

NheI/XhoI digested pcDNA3.1(-)mychisB with HpaI/XhoI digested PCR product 1 (amplified from pT7.7MDMX using primer pair 5'-GCTAGCTGTTTCGTTGTTGGGCCTTGA-3'/5'-

CTCGAGTGCTATAAAAACCTTAATAACCAGCTGA-3') and NheI/HpaI digested PCR product 2 or 3 (amplified from MCF-7 cDNA using following primer pairs (PCR 2, HDMXP1 5'-GGGAGGCCGGAAGTTGCG-3'/5'-CAGTGATATCAGACGTGGAGAGAGAATGGTTAAC-3'; PCR 3, HDMXP2 5'-GCTAGCAGTTGGAGGTTGGAGCGTGC-3'/5'-CAGTGATATCAGACGTGGAGAGAGAATGGTTAAC-3')) to give pP1-HDMXmh and pP2-HDMXmh respectively. pP1-HDMX and pP2-HDMX were created using site-directed mutagenesis to introduce a stop codon immediately 5' of the mychis tag. p21-luc reporter vector and pC53SN3 expressing human p53 were from Bert Vogelstein. pCMVDDp53 was from Moshe Oren. pHDM2 (pCMVMDM2) containing cDNA for human MDM2 was from AJ Levine. pHis<sub>6</sub>Ub was made available by S. Mittnacht. HDM2luc01 reporter vector was described previously (21), as was the Flag-p53 expression vector (43).

*RNAi, transfections and reporter gene assays-* RNAi-mediated knockdown of *HDMX-P2* was performed using the following siRNA (5'-GCUUGGACGAUUCUUACUCdTdT-3'/3'-dTdTTCGAACCUGCUAAGAAUGAG-5') obtained from Qiagen. Appropriate control siRNAs, as described by (44) were as follows; HDMX-P2ctrl1 containing 4 nucleotide mismatch in seed region (5'-GCUUGGACGAUUCUUAGCAAUCdTdT-3'/3'-dTdTTCGAACCUGCUAUCGUUAG-5'); HDMX-P2ctrl2 containing 4 nucleotide mismatch in central region (5'-GCUACGGUGAUUCUUACUCdTdT-3'/3'-CGAUGCCACUAAGAAUGAG-5'; 75 nM). siRNA to the HDMX coding region was from Ambion (MDM4, #121374). p53 siRNA was obtained from Qiagen (Hs\_TP53\_9 HP validated; 25 nM). Negative control siRNA no. 1 (Ambion) was used at the appropriate concentration for experimental controls, and total siRNA concentration was equalized in all

samples using negative control siRNA. siRNA was transfected for 4 h using INTERFERin reagent (Polyplus Transfection). The construction of lentiviral vectors expressing specific shRNAs and the production of lentivirus particles has been described recently (45). The target sequence for *HDMX-P2* mRNA was the same as the siRNA mentioned above. The sequences targeting human and mouse p53 have been published (46,47). For transfection of plasmid DNA Lipofectamine 2000 (Invitrogen) was used. Unless stated otherwise reporter assays were performed in triplicate, and assayed 48 h after transfection using a Dual-Glo<sup>TM</sup> luciferase assay (Promega) on cells transfected in 96-well plates, with normalization to *Renilla* luciferase expressed from pRLSV40 (Promega). Data pooled from at least two independent experiments is shown as mean ± SEM.

*In vivo ubiquitination assay-* 24 h post-transfection, H1299 cells were exposed to 25 μM MG132 (Sigma) for 4 h before protein was extracted by denaturing urea buffer and quantified as described above. 20 μg of total extracted proteins were analyzed by direct Western blotting and 120 μg proteins were used to extract His<sub>6</sub>-ubiquitinated conjugates as described in (48).

*In vitro transcription and translation-* RNA was transcribed from 3.3 μg linearized HDMX expression vectors using T7 RNA polymerase (Promega). Template DNA was removed by digestion with RQ1 RNase-free DNase (Promega) before RNA purification using RNAbee reagent (Biogenesis Inc.). Indicated amounts of RNA were used as templates in *in vitro* translation reactions using nuclease-treated rabbit reticulocyte lysate (Promega). 10% of reactions were separated by SDS-PAGE before HDMX expression levels were determined by Western blotting.

*Chromatin Immunoprecipitation-* the protocol is adapted from (49). Cells were cross-linked in 1% formaldehyde for 30 min at room temperature, after which cross-linking was stopped by adding glycine to an end concentration of 125 mM. Cells were put on ice, rinsed twice with ice cold PBS, and scraped in HEPES lysis buffer (10 mM HEPES, pH 7.6; 1% NP40, 1 mM EDTA, 400 mM NaCl, 10% glycerol; supplemented with protease and phosphatase inhibitors). Lysates were centrifuged at 11000 rpm, 10 min at 4°C. Pellets were resuspended in 500 μl HEPES lysis buffer, and spun again for 5 min, 11000 rpm, 4°C.

Pellets were resuspended, and left on ice for about 30 min, and subsequently sonicated in Bioruptor (30'' on, 30'' off; 2 x 10 min; high power). Insoluble material was removed by centrifugation at 13000 rpm, 10 min at 4°C. Supernatant was transferred to new tube, and diluted 1:1 with HEPES dilution buffer (10 mM HEPES, pH 7.6, 1 mM EDTA, 10% glycerol; supplemented with protease and phosphatase inhibitors). Aliquots were taken and stored at 4°C to represent input material. 300 µl of chromatin solution was used for immunoprecipitation, with a combination of DO-1 and PAb1801 (Santa Cruz Biotechnology) anti-p53 antibodies (4 µg antibody/IP; bound to 10 µl protein G beads) for human cells and FL-393 rabbit polyclonal antibody (Santa Cruz Biotechnology; 2 µg/IP; bound to 10 µl protein A beads) for mouse cells. IPs were performed overnight at 4°C, in a total volume of 400 µl, in presence of 0.1 µg/µl BSA. Beads were then washed (x3) in wash buffer (10 mM HEPES, pH 7.6, 0.5% NP40, 1 mM EDTA, 200 mM NaCl, 10% glycerol, supplemented with protease and phosphatase inhibitors). Beads were eluted for 20 min at room temperature (rotating) in elution buffer (1% SDS, 0.1 M NaHCO<sub>3</sub>), after which beads were spun down, and supernatant transferred into a new tube. 16 µl 5M NaCl was added, and cross-linking of samples (including input chromatin; 50 µl + 350 µl elution buffer) was reversed for 4-5 h 65°C. Chromatin was purified by phenol-chloroform-isoamylalcohol (25:24:1) extraction followed by chloroform: isoamylalcohol (24:1) extraction and subsequent ethanol precipitation in the presence of 2 µg/µl glycogen. Pellets were dissolved in milliQ water, and these chromatin samples were used for analysis by qPCR. Primers used to amplify the specific genomic regions are given in supplementary table 1.

## RESULTS

*The HDMX gene contains a functional p53-responsive promoter in intron 1-* as an initial step in the analysis of the regulation of *HDMX* gene expression we used BLAST to search human EST databases for mRNAs which contain the first coding exon of *HDMX*; exon 2. In addition to ESTs which matched the published *HDMX* cDNA sequence (50), two sequences included at their 5' end a novel exon spliced into the start of exon 2. Both ESTs had been

identified from a thymus library using a method that aims to find the extreme 5' ends of cDNAs; of the two, DB137351 extended furthest in the 5' direction. This exon is located in intron 1, and we have termed it exon 1β (Fig. 1A). Global genomic profiling previously identified a p53-binding region in intron 1 (35). We identified a good match to the p53-binding site consensus sequence (51) 151 b.p. 5' to the likely 5' limit of exon 1β (Fig. 1A). Thus, this bioinformatics analysis suggested that *HDMX* might contain a second, p53 responsive promoter in intron 1, analogous to the P2 promoter in the *HDM2* gene (Fig. 1A). To determine whether this putative *HDMX-P2* promoter is functional we cloned 1334 b.p. of genomic promoter sequence into a luciferase reporter vector and tested the activity of this construct (HDMXP2luc01) in the MCF-7 cell line (Fig. 1B). These cells express endogenous wild-type p53 that becomes activated in response to DNA transfection. The promoter showed robust activity, which was approximately 25% of that of the highly p53-responsive *p21<sup>WAF1</sup>* promoter. *HDMX-P2* promoter activity was reduced by >85% when p53 protein expression was inhibited using siRNA. *HDMX-P2* activity in MCF-7 cells is strictly dependent upon an 80 b.p. region that includes the predicted p53 response element (p53-RE<sup>1</sup>) (compare HDMXP2luc08 with HDMXP2luc05 in Fig. 1Ci). Similar findings were obtained when a subset of these vectors were tested in the p53 null H1299 cell line, in the absence (open bars) or presence (solid bars) of co-transfected p53-expression vector (Fig. 1Cii). A targeted 3 b.p. substitution in the predicted p53-RE reduced promoter activity in MCF-7 cells as effectively as was achieved by inactivation of endogenous p53 using a dominant negative p53 fragment (Fig. 1D). Activation by exogenous p53 transfected into H1299 cells was also completely abrogated by this mutation (supplemental figure S1A). Therefore, the predicted p53-RE is indeed essential for p53-dependent *HDMX-P2* promoter activity.

P53-dependent transcriptional activity can be activated in response to a wide range of cellular stresses and pharmacological agents. We therefore examined the effects of two different p53 activating agents on *HDMX-P2* promoter activity in MCF-7 cells (Fig. 1E). 5-Fluorouracil (grey bars) and Nutlin-3 (open bars) both increased its activity in MCF-7, through a p53-RE-dependent mechanism. Finally, we

noted that the p53-RE in the *HDMX-P2* promoter was as good a match to the p53 consensus sequence as that found in the highly p53-responsive *p21<sup>WAF1</sup>* promoter, and better than weaker response elements found in, for example, the *BAX* promoter. We, therefore, examined the relative p53-responsiveness of *HDMX-P2* promoter compared to other p53-responsive promoters (supplemental figure S1B). The *HDM2-P2* promoter contains two p53-REs and is highly responsive to low levels of transfected p53. *HDMX-P2* and *p21<sup>WAF1</sup>* promoters showed comparable fold induction by p53, this being approximately two fold greater than the activation of the *BAX* promoter.

*Genotoxic, oncogenic and pharmacological p53-activating signals induce transcription from the endogenous p53-responsive HDMX-P2 promoter-* the previous section clearly demonstrates that synthetic reporter constructs containing the novel *HDMX-P2* promoter region do exhibit p53-dependent transcription of the reporter gene when transfected into cells. This is consistent with similar findings reported by Li *et al.* in different experimental systems (36). It has also been shown that p53 can bind to chromatin in this region of the endogenous *HDMX* gene (35,36). However, in order to demonstrate that this is indeed a functional promoter in the context of endogenous chromatin, it was necessary to establish whether *HDMX* mRNA is transcribed from the *HDMX-P2* promoter in response to p53-activating signals.

Transcript-specific PCR for mRNAs containing both exon 1 $\beta$  and *HDMX* coding sequence-containing exons can be used to identify transcripts derived from the *HDMX-P2* promoter. This approach selectively identifies these transcripts because mRNA transcribed from the constitutive P1 promoter of *HDMX* contains exon 1 spliced directly to exon 2; exon 1 $\beta$  being skipped (50). Furthermore, in our EST analysis, no transcripts were detected which contained exon 1 $\beta$  spliced 3' to another exon. To determine whether p53 can induce activity of the endogenous *HDMX-P2* promoter we made use of the p53 null SAOS-2 cell line containing p53 under the control of a doxycycline-inducible promoter (37) (Fig. 2A). Induction of p53 synthesis in these cells resulted in a robust increase in the expression of *p21<sup>WAF1</sup>* and *HDM2*, the products of known p53-responsive genes. At the mRNA level, induction of p53 had no detectable effect on the abundance of total

*HDMX* mRNA, although there was a very clear increase in the abundance of the mRNA product of the *HDMX-P2* promoter, which was not detectable in the absence of p53. Thus, as we have discussed, induced *HDMX-P2* transcript levels are likely to be relatively low compared to the abundance of the constitutive P1 promoter-derived transcript. Incidentally, two bands are detected by this *HDMX-P2* mRNA PCR in SAOS-2, since the PCR spans exon 6, which can be alternatively spliced to produce the *HDMX-S* variant (52). SAOS-2 cells mainly express *HDMX-S*, while e.g. ZR75-30 and MPE600 cells predominantly express full length *HDMX* mRNA (Fig. 2B). Chromatin immunoprecipitation analysis confirmed that p53 protein was recruited to the endogenous *HDMX-P2* promoter in these SAOS-2/p53 cells, comparably to its recruitment to the *HDM2-P2* and the *p21<sup>WAF1</sup>* promoters (Fig 2A, lower panel).

We next examined whether *HDMX-P2* promoter-derived transcripts are synthesized in cells in response to activation of endogenous p53 in cells, by exposing a panel of wild-type p53-expressing breast cancer cell lines to either Nutlin-3 or Etoposide (Fig. 2B). In normally proliferating MCF-7 cells *HDMX-P2* transcripts were virtually undetectable by our RT-PCR assays. Nutlin-3 induced a robust increase in the abundance of this mRNA with kinetics consistent with it following the increase in p53 protein abundance. Peak induction of *HDMX-P2* transcripts was observed after 8 h treatment. In two other wild-type p53-expressing breast cancer lines, ZR75-30 and MPE600, detectable amounts of the *HDMX-P2* transcripts were present in normally proliferating cells; nevertheless both lines showed a similarly robust induction of *HDMX-P2* transcripts in response to either Nutlin-3 or Etoposide (Fig. 2B). There was no such induction in p53-null SAOS-2 cells (Fig. 2B). The *HDMX-P2* transcripts were also detectable in proliferating testicular germ cell tumor (TGCT) lines, in which they were strongly induced by Nutlin-3 (supplemental figure S2A). Of note, when the data in this figure are compared to those of Li *et al.* (36), whose analysis was completely based on TGCT cells, both studies show that Nutlin-3 causes a modest increase in total *HDMX* transcripts in 833 KE cells, but not N-TERA-2. However, our transcript-specific analysis shows that *HDMX-P2* promoter derived transcripts are, in fact, robustly induced in both cells lines. In all the

breast cancer and TGCT lines, Nutlin-3-mediated activation of p53 also caused a modest increase in HDMX protein abundance. This increase is not seen upon Etoposide-treatment, most likely because DNA damage triggers the HDM2-mediated degradation of HDMX proteins (53,54).

Subsequent experiments using siRNA to p53 confirmed that both the basal and inducible expression of *HDMX-P2* transcripts in these breast cancer lines and other wild-type p53 expressing cells, such as 92.1 uveal melanoma cells, is dependent upon p53 (Fig. 2C, supplemental figures S2B,F and data not shown). Chromatin immunoprecipitation experiments in VH10 (primary foreskin fibroblasts) and MPE600 showed a cell line dependent increase in the association of p53 with *HDMX-P2* promoter regions in response to Nutlin-3 (Fig. 2D). We next performed a number of experiments in order to determine the generality of *HDMX-P2* promoter activation in response to alternative p53-activating stresses, and in different cell lines. Oncogenic stress is a key activating signal, which can occur through increased expression of the HDM2 inhibitor, p14<sup>ARF</sup>. Using the U2OS-derived NARF cells ((55), a kind gift from Gordon Peters), in which p14<sup>ARF</sup> expression is inducible by IPTG, *HDMX-P2* transcripts are clearly induced with kinetics that follow the stabilization of p53 protein (Fig. 2E). Other p53-activators such as Cisplatin (Fig. 2F), as well as Neocarzinostatin, Leptomycin B and RITA (supplemental figures S2E,F) also clearly induce transcription from the *HDMX-P2* promoter in multiple cell lines that express wild-type p53. In general, from these and other (e.g. supplemental figure S5C) experiments we find that compared to tumor cell lines, untransformed cells show a relatively modest increase of *HDMX-P2* mRNA in response to p53 activators, despite other p53-response mRNAs such as *HDM2-P2* being relatively highly induced. It is also noteworthy that, in many examples where *HDMX-P2* transcripts are robustly induced, this p53-induced transcription of *HDMX* is undetectable when total *HDMX* transcripts are analyzed. Furthermore, even when induced alternative splicing results in a decrease in full length *HDMX* transcripts, in response to Leptomycin B for example, *HDMX-P2* mRNA transcripts are robustly induced, albeit in the alternatively spliced form.

*Transcriptional regulation of HDMX by p53 is evolutionarily conserved-* our previous analysis of ESTs containing murine *mdmx* also identified transcripts containing an exon 1 $\beta$  (6). This exon shows limited homology to the human exon 1 $\beta$ , and does not contain an in-frame ATG. Nevertheless, the genomic region 5' to the murine exon 1 $\beta$  does contain a potential p53-response element (Fig. 3A). In order to determine whether exon 1 $\beta$  *mdmx* transcripts are inducible by p53, we infected MEFs with lentiviruses, expressing control or p53-specific shRNA, prior to exposing them to Nutlin-3 (Fig. 3B). Nutlin-3 caused the expected increase in p53 protein abundance, which was reduced by the p53 shRNA. RT-PCR to detect total *mdmx* mRNA again detected two bands, due to alternate splicing of exon 6 (52). There was small but detectable effect of p53 activation on the abundance of the full length *mdmx* mRNA transcripts, the p53-dependency of this increase being confirmed in a separate experimental system (supplemental figure 3B). In contrast, *mdmx-P2* promoter-derived transcripts containing exon 1 $\beta$  were very clearly induced by Nutlin-3, again in a p53-dependent manner. qRT-PCR showed that the abundance of *mdmx-P2* promoter derived transcripts increased by approximately 30-fold after 7 h of Nutlin-3 treatment in these cells (Fig. 3B). Ionizing radiation (supplemental figure S3A) and Etoposide (supplemental figure S3B) also cause p53-dependent induction of this transcript. In a separate experimental system (Fig. 3C), we showed that *mdmx-P2* derived transcripts failed to be induced by Nutlin-3 in *p53*<sup>-/-</sup> MEFs, whereas they were induced in wild-type p53-expressing B16F10 mouse melanoma cells. Chromatin immunoprecipitation experiments clearly demonstrate recruitment of p53 to the predicted *mdmx-P2*-promoter region in Nutlin-3 treated B16F10 cells. Finally, we investigated whether p53-activating stress induces the expression of *mdmx-P2* derived mRNA in normal tissues *in vivo*. Figure 3D shows that *mdmx-P2* mRNA transcripts are detectable in the bone marrow of C57/BL6 mice, and are clearly induced in response to 4 Gy of ionizing radiation. Together these experiments provide strong evidence that the murine *mdmx* gene also contains a functional p53-responsive P2-promoter in intron 1, and *mdmx-P2* transcripts are clearly induced in response to diverse p53-activating signals.

*mRNA transcribed from the human HDMX-P2 promoter is translated into HDMX-L: a long, functionally distinct, form of HDMX-* the mRNAs transcribed from the P1 and P2 promoters of human *HDMX* differ in the inclusion at the 5' ends of either exon 1 or exon 1 $\beta$  respectively. Exon 1 contains two potential upstream open reading frames (uORFs) which could potentially suppress translation of HDMX protein. Indeed, as we have already discussed, for the comparable *HDM2* transcripts, *HDM2-P2*-derived mRNA (which lacks any uORFs) can be translated up to eight-fold more efficiently than the *HDM2-P1* mRNA (22-24). Exon 1 $\beta$  of *HDMX* also lacks any out of frame uORFs, but does contain an in-frame ATG which, if utilized as a translation start site, would result in the synthesis of a long form of HDMX protein with an additional 18 amino acids at its N-terminus (Fig. 1A). We therefore performed a quantitative and qualitative analysis of the translation of these two *HDMX* transcripts. Constructs containing either exon 1 or exon 1 $\beta$  5' to exons 2-11 (pP1-HDMX and pP2-HDMX, respectively) were generated, transcribed *in vitro*, and equal amounts of mRNA added to *in vitro* translation reactions. We also examined mRNA from pP2-HDMX $\Delta$ ATG1, in which the normal translation initiation site in exon 2 was mutated (Fig. 4A). Approximately seven-fold more protein was translated from the pP2-HDMX mRNA compared to pP1-HDMX mRNA. Furthermore, the protein product of pP2-HDMX-derived mRNA had a slightly reduced mobility on SDS-PAGE compared to HDMX translated from pP1-HDMX, and furthermore, the product is still present upon deletion of the AUG in exon 2. Essentially the same differences between the P1- and P2-promoter synthetic transcripts were obtained when expression vectors were transfected into human cancer cell lines (supplemental figure S4A; note in this experiment the proteins had a C-terminal tag to distinguish them from endogenous cellular HDMX proteins). Thus, when expressed, the mRNA transcribed from the P2 promoter is efficiently translated from the ATG in exon 1 $\beta$  to generate a long form of HDMX, which has 18 additional amino acids at its N-terminus, compared to HDMX. We have termed this novel protein HDMX-L.

We set out to determine whether the presence of these additional amino acids has any consequence for HDMX-L regulation or function. A key point at which HDMX function

is regulated is through its subcellular localization; in many proliferating cells HDMX is primarily cytoplasmic; genotoxic stress results in its ATM and 14-3-3 protein-dependent relocalization to the nucleus, where it can function to inhibit p53 (27,56). Supplemental figure S4B shows that both HDMX and HDMX-L have the same subcellular distribution in both the absence and presence of etoposide-induced DNA damage. A second key point at which HDMX is regulated is through its rate of degradation via HDM2-dependent ubiquitination. HDMX and HDMX-L showed no differences in their HDM2-dependent destruction pathway, either in the absence or presence of genotoxic stress (supplemental figures S4C and S4D).

HDMX exerts its functions through two key proteins, HDM2 and p53. HDMX:HDM2 heterodimers function as E3-ubiquitin ligases for p53, and thus HDMX can promote HDM2-dependent ubiquitination of p53 when HDM2 protein concentrations are limiting. This effect of HDMX can be seen in Fig. 4B (lane 5, left panel). Expression of HDMX-L from the pP2-HDMX vector had the same effect (lane 6); multiple repeats of this experiment demonstrated both HDMX-L and HDMX function comparably in this assay. Consistent with the formation of heterodimers, both HDMX and HDMX-L also promote HDM2 auto-ubiquitination, and are themselves ubiquitinated in the presence of HDM2 (Fig. 4B). The interaction between HDMX and HDMX-L with p53 was then determined by immunoprecipitation analysis. N-terminally HA-tagged HDMX and HDMX-L were precipitated with anti-HA antibody and the amount of FLAG-tagged p53 that was co-precipitated determined. HDMX-L consistently pulled down less p53 protein than did HDMX (Fig. 4C, left panel). In the reciprocal analysis (Fig. 4C, right panel), immunoprecipitation of p53 clearly pulled down less HDMX-L than HDMX. These results imply that the 18 amino acid N-terminal extension of HDMX-L interferes with efficient interaction between p53 and HDMX in cells. Through its direct interaction with p53, HDMX inhibits the p53-dependent transcription from p53-responsive promoters. We, therefore, examined whether the reduced p53-binding efficacy of HDMX-L affects its p53-inhibitory activity (Fig. 4D). HDMX, expressed from pP1-HDMX, caused a dose-dependent reduction in the p53-dependent transcription from the *p21<sup>WAF1</sup>* promoter (open

bars); complete inhibition of p53-activity was not observed in this assay as HDMX requires either HDM2 binding, or stress-induced 14-3-3 binding for its optimal nuclear localization that is required for its inhibition of p53. In contrast, HDMX-L expressed from the pP2-HDMX construct failed to have any effect on p53-dependent transcription in this assay. Together these data demonstrate that, compared to HDMX translated from the constitutive P1 promoter, HDMX-L translated from the p53-inducible P2 promoter retains the ability to cooperate with HDM2 in the ubiquitination of p53, but is compromised in its ability to inhibit p53-dependent transcription through direct interaction with the transactivation domain of p53.

We subsequently established MCF-7 cell line clones stably over-expressing HDMX or HDMX-L (Fig S4F) and vector-only cell lines as controls; distinct clones expressing equivalent amounts of the two proteins being selected for further analysis. Primarily we have used the clones HX/C3 and HX-L/C11 that exhibit moderate expression of exogenous HDMX/HDMX-L, but HX/C6 and HX-L/C10 have also been compared with similar results. Initially we investigated the p53 response upon treatment with Nutlin-3 for 6 h by determining the induction of p53 target genes. As shown in Fig. 4E, activation of *PUMA*, *HDM2-P2* and *p21<sup>WAF1</sup>* is compromised in HDMX-expressing MCF-7 cells compared to vector-transfected controls. In HDMX-L expressing cells, *HDM2-P2* induction is similarly compromised, whereas there is an intermediate inhibitory effect on *PUMA* induction and *p21<sup>WAF1</sup>* induction was slightly elevated compared to controls. We also investigated the *SURVIVIN* gene, the abundance of which was repressed by Nutlin-3 to a similar extent in all three lines and found a slight decrease which was comparable in the different cell lines. This effect was quite modest, presumably because the 6 h time-point used is too short for any transcriptional repression of the *SURVIVIN* gene to result in clear effects on the abundance of its mRNA.

Together, all these results indicate that, compared to HDMX, HDMX-L is compromised in its ability to suppress the p53-response. To determine whether this effect could be recapitulated in a biological response, we determined the effect of Nutlin-3 and Actinomycin D on cell proliferation and survival, using both short term (72 h) cell

proliferation assays (Fig. 4F) and long-term colony survival assays (Fig. 4G). In both assays, HDMX over-expression conferred protection to these p53-activating compounds compared to vector-transfected controls, while MCF-7 cells expressing HDMX-L were also protected, but to a consistently lesser extent than the HDMX expressing cells. These results indicate that, like in the luciferase assays, the HDMX-L protein has reduced capacity to inhibit p53 activity and p53-induced anti-proliferative responses.

*The role of p53-dependent transcription of HDMX in the feedback control of p53-* from the above data it is clear that transcription from the *HDMX-P2* promoter is inducible by a wide range of p53-activating stress in diverse human and murine cell types. We, therefore, wished to establish the contribution of this transcript to the abundance of HDMX proteins, and the regulation of the p53 pathway, in normally proliferating and stressed cells. To do this we developed RNA interference reagents that would specifically target the *HDMX-P2* transcript by recognizing sequences within the 130 b.p. unique to exon 1 $\beta$ . siRNA oligonucleotides were screened in MCF-7 cells in the absence or presence of p53-activating signals. One of the tested siRNAs most effectively reduced the abundance of p53-induced *HDMX-P2* mRNA. Two further control siRNAs were synthesized based on this *HDMX-P2* siRNA, which had 4 base pair mismatches in the seed and central regions respectively. Supplemental figure S5A shows that whilst none of the control siRNAs affect either *HDMX-P2* transcript levels, or p53 protein abundance, the *HDMX-P2* siRNA substantially reduces radiation-induced *HDMX-P2* transcripts (Nutlin-3 experiments are shown in Fig. 6). Exposure of MCF-7 cells to 5 Gy ionizing radiation causes a substantial decrease in the abundance of HDMX protein (Fig. 5A, S5A), due to the activation of its ATM and HDM2-dependent degradation (note that we have used the term HDMX to refer to the endogenous ~75 kDa HDMX proteins, which may consist of both HDMX and HDMX-L). This decrease is more pronounced in the *HDMX-P2* siRNA-transfected cells than those transfected with control siRNA (Fig. 5S, S5A); time-course analysis of multiple repeated experiments (Fig. 5A, western blot and quantification) clearly demonstrates that, in the first 2-4 hours after irradiation, HDMX protein abundance drops rapidly, before leveling out at 6

h and beginning to increase again at 8 h. *HDMX-P2* transcripts are upregulated during this time frame, and the siRNA experiments clearly demonstrate that they are responsible for this early recovery of HDMX protein abundance in these cells. MCF-7 and MPE600 cells infected with a lentivirus expressing a shRNA targeting the same sequence also showed a more pronounced reduction in HDMX in response to etoposide, than did control shRNA-expressing cells (Fig. 5B). Interestingly, the normal fibroblast line MRC5-hTERTneo did not detectably induce *HDMX-P2* transcripts in response to 5 Gy irradiation, and HDMX protein levels remained low for at least 24 hours after radiation exposure (supplemental figure S5C). Therefore, in cells in which the *HDMX-P2* transcript is induced in response to genotoxic stress, it makes a clear contribution to the abundance of HDMX protein, and in particular the rate at which it recovers after its initial stress-induced degradation. This has a clear consequence on the abundance of p53 in response to DNA-damaging stress. In both of the breast cancer cell lines the magnitude of the initial stabilization of p53 is not substantially affected by *HDMX-P2* siRNA (Fig. 5A, B), nor is the p53-dependent G<sub>1</sub> arrest response increased (supplemental figure S5D). However, p53 protein stabilization is prolonged, levels remaining elevated for 24 h following etoposide treatment in *HDMX-P2* knockdown cells, whereas they begin to drop towards baseline levels by 8 h in control cells (Fig. 5B). The degradation of p53 during the period following its initial stabilization in response to ionizing radiation is also delayed in *HDMX-P2* siRNA-transfected MCF-7 cells (Fig. 5A). Together, these findings are consistent with a role for HDMX and HDMX-L in promoting the HDM2-dependent degradation of p53 during the attenuation phase of the stress response.

The above breast cancer cell lines undergo a primarily cell cycle arrest response to p53 activation (e.g. supplemental figure S5D). In order to examine the role of *HDMX-P2* transcripts in p53-dependent pro-apoptotic responses, we examined the testicular germ cell tumor line, N-TERA-2, which are highly sensitive to apoptosis induced by p53-activating DNA damaging agents (57) or Nutlin-3 (58). Furthermore HDMX is known to be important in regulating p53 in these cells, as siRNA which targets all *HDMX* mRNA transcripts results in the stabilisation of p53, and the upregulation of

p53-responsive proteins in the absence of any other p53-activating signal (36). We therefore transduced N-TERA-2 with lentiviral constructs expressing shRNA targeting *HDMX-P2* mRNA or *p53* or both, or a control shRNA, and selected for puromycin-resistance. Transduced cells were treated with Etoposide for 2 h after which medium was replaced. Cells were harvested at several time-points to analyze protein and RNA expression. As shown in Fig. 5C, Etoposide does increase *HDMX-P2* levels in these cells, and the shRNA reduces this induction. Etoposide causes HDMX protein levels to decrease, both in the control and *HDMX-P2* knockdown cells. This reduction is slightly greater in the *HDMX-P2* knockdown cells demonstrating that induction of *HDMX-P2* transcripts does diminish the degree of reduction of HDMX protein abundance that occurs in these treated cells. p53 is stabilized by Etoposide in control shRNA transduced cells and p53 levels remained high for at least 24 h (Fig. 5C). In comparison, p53 abundance is more strongly increased by Etoposide in the *HDMX-P2* shRNA transduced cells. In these N-TERA-2 cells p53-induced *HDMX-P2* expression is also clearly important in regulating the degree of upregulation of p53-responsive proteins; PUMA and p21<sup>WAF1</sup> being more strongly upregulated in the *HDMX-P2* depleted cells. So, as was the case in the breast cancer cells, these data demonstrate that the upregulation of *HDMX-P2* transcription is also important in attenuating the p53-response to DNA damage in this TGCT cell line.

DNA damaging agents can have p53-independent effects on cell proliferation and survival (e.g. see (57)). In order to clearly understand the role of p53-inducible *HDMX-P2* promoter activity on the cellular response to p53 activation, we examined the effects of RNAi to *HDMX-P2* mRNA in cells treated with Nutlin-3, as the effects of this compound are largely p53-dependent. Treatment of MCF-7 cells caused a modest, up to two-fold, increase in the abundance of HDMX protein (Figs. 2B, 6A). This increase is blocked by the *HDMX-P2* siRNA (Fig. 6A; western blot & quantification). *HDMX-P2* siRNA also caused a reproducible enhancement of the increase in p53 protein abundance in response to Nutlin-3 (Fig. 6A, western blot and quantification). MCF-7 cells infected with a lentivirus expressing a shRNA targeting the same sequence also failed to demonstrate an increase in HDMX in response

to Nutlin-3 and the Nutlin-3-induced increase in p53 protein abundance was enhanced (Fig. 6B). Similar effects of the shRNA were seen in Nutlin-3 treated MPE600; cells expressing *HDMX-P2* shRNA showed no difference in basal HDMX or p53 protein abundance, but the Nutlin-3-induced reduction of HDMX and stabilization of p53 was enhanced (Fig. 6B). Together these experiments clearly demonstrate that, in the breast cancer cells in which the *HDMX-P2* transcript is induced in response to p53-activation by Nutlin-3, it makes a demonstrable contribution to the abundance of HDMX protein. In contrast, when we examined MRC5-hTERTneo cells, Nutlin-3 failed to detectably induce *HDMX-P2* mRNA transcripts. In these cells Nutlin-3 caused a reduction, rather than increase, in HDMX protein levels (supplemental figure S6B), as has been reported by earlier publications using similar non-transformed fibroblast cell lines (29,59).

We then considered the effect of *HDMX-P2* RNAi on the cellular response to Nutlin-3 in the breast cancer cells. In contrast to the effects on p53 protein abundance, we did not reliably detect any consistent effects of *HDMX-P2* knockdown on the abundance of HDM2, p21<sup>WAF1</sup> or PUMA (Fig. 6A, 6B, S6A & not shown). When sub-confluent monolayers of MCF-7 cells were exposed to Nutlin-3, *HDMX-P2* siRNA did not enhance Nutlin-3-induced cell cycle arrest or apoptosis (supplemental figure S6C), or long-term survival (not shown). However, when MCF-7 cells were stressed by plating at low density, their ability to form viable colonies was reduced by prior transfection with *HDMX-P2* siRNA; colony formation being further reduced by the combination of the siRNA with Nutlin-3 (Fig. 6C).

As mentioned above, the N-TERA-2 cells are prone to enter apoptosis upon activation of p53 while MCF-7 and MPE600 cells are more likely to enter a cell cycle arrest. Therefore, we tested whether N-TERA-2 would also show altered p53 activation upon Nutlin-3 treatment in *HDMX-P2* knockdown cells compared to controls. Cells transduced with lentiviral vectors expressing shRNA as in Fig. 5C were treated with 10  $\mu$ M Nutlin-3 continuously for 20 h, and RNA and protein lysates analyzed. *HDMX-P2* transcripts were strongly induced in the control cells, and *HDMX-P2* specific shRNA reduces the abundance of these transcripts (supplemental figure S6D). This figure also shows clearly that *HDMX-P2* expression is dependent on p53 in

these cells. Both basal and Nutlin-3 induced HDMX protein levels were marginally reduced by the *HDMX-P2* shRNA, however no differences in increase of p53 or targets were observed be found, except when p53 shRNA was also expressed (Fig. S6D, similar results were obtained with 6 h or 8 h Nutlin-3 exposure, not shown). Nevertheless, compared to the control cells, the *HDMX-P2* shRNA expressing cells did exhibit slightly higher p53-dependent apoptosis, as determined by a PARP cleavage assay, when treated with Nutlin-3. It is possible that the extended treatment with this concentration of Nutlin-3 results in a near maximal activation of p53 that is rather insensitive to changes in HDMX abundance. Therefore, similarly to the experiment shown in Fig. 5B with the breast cancer cells, we exposed N-TERA-2 cells to Nutlin-3 for only 2 h before washing it off and assaying molecular markers of the p53 response at subsequent time points (Fig. 5C). As before, *HDMX-P2* transcripts are induced by Nutlin-3, and this induction is reduced by *HDMX-P2* shRNA. Strikingly, in control shRNA transduced cells p53 levels are initially induced only very transiently and decrease rapidly towards baseline levels once the drug is removed (though does rise again somewhat at 24 h) (Fig. 6D). In the *HDMX-P2* knockdown cells the induced levels of p53 at the 2 h time point are clearly higher than in control cells and, whilst p53 protein abundance does decrease upon removal of the Nutlin-3, it remains elevated above baseline levels for 8 hours. Furthermore, the p53 targets p21<sup>WAF1</sup> and PUMA are more strongly induced in the *HDMX-P2* knockdown cells compared to control cells, though HDM2 levels are more comparable. These effect of the *HDMX-P2* shRNA on the p53-response to Nutlin-3 in N-TERA-2 cells occur despite it having only very modest effect on total HDMX protein abundance, there only being a small increase in HDMX at 2 h in the control cells that is absent in the *HDMX-P2* knockdown. One possibility that is suggested by our data is that changes in the HDMX to HDMX-L ratio in these cells would occur, and these could contribute to the observed altered p53 response.

To investigate whether these effects of manipulating *HDMX-P2* transcript expression on molecular aspects of the p53 response translate to an altered phenotypic response, the shRNA-expressing N-TERA-2 cells were also seeded for long-term (colony assays) and short-term growth

assays, to determine their sensitivity to Nutlin-3 treatment. Based on the previously shown experiments, we reduced the concentrations of Nutlin-3 used to 2 and 4  $\mu\text{M}$ , and treated the cells for the colony assays for only 24 h before removing it and replacing the medium. The results clearly show that inhibiting *HDMX-P2* transcript expression sensitizes N-TERA-2 cells for Nutlin-3 induced inhibition of long term cell viability (Fig. 6E). Similarly, a multiple repeats of a short-term growth assay shows that the *HDMX-P2* knockdown cells are more sensitive for Nutlin-3 induced cell death (Fig. 6F). In both cases this effect of the *HDMX-P2* shRNA is entirely p53-dependent. Together, these results clearly demonstrate that the induction of HDMX-L expression in response to p53 activation suppresses the p53-response upon Nutlin-3 treatment, with associated effects on cell proliferation and survival.

## DISCUSSION

The activation of a p53-dependent transcriptional program is a key component of the cellular response to a diverse range of cellular stress signals. Key p53-responsive genes such as *p21<sup>WAF1</sup>* and *PUMA* initiate the cell cycle arrest and pro-apoptotic responses; these, and a wide range of other transcriptional targets of p53, implicate the p53 stress-response pathway in tumorigenesis as well as other key aspects of human physiology and pathology, e.g. (60,61). In proliferating cells p53 protein is synthesized and has the potential to be active as a transcription factor (62). Cell proliferation is dependent on its abundance and activity being maintained at low levels via a dynamic equilibrium with its negative regulatory proteins HDM2 and its paralog and hetero-dimeric protein partner, HDMX (6,7). A general, if not obligate, process whereby p53 is activated in response to stress involves the relief of the negative regulation of p53 by HDM2 and HDMX (7,63). The precise mechanisms whereby this occurs depends on the nature of the stress; e.g. DNA single strand breaks trigger the ATM-dependent phosphorylation of p53, HDM2 and HDMX, promoting both p53 activation, and the HDM2-dependent destruction of HDM2 and HDMX (7,28), whereas stresses that suppress transcription, e.g., experimentally using low dose Actinomycin D, result in the binding and inhibition of HDM2 by ribosomal proteins, as well as the HDM2-dependent degradation of

HDMX (64). In these and other studies HDMX, and more specifically the precise stoichiometry between p53, HDM2 and HDMX within cells (65), is revealed as a critical regulator of the response, potentially through either the ability of HDMX to bind and inhibit p53 directly, or through its dimerization with HDM2 and regulation of HDM2-dependent ubiquitination of p53.

Factors influencing the abundance and activity of HDM2 and HDMX, therefore, potentially influence both the maximal intensity and duration of the p53-dependent transcriptional response to a particular stress. Regulation of the intensity of the response can be critical, as p53-responsive genes differ in their sensitivity to activation by p53, for example due to variations in the sequences of the p53-response elements in the promoters of the CDK inhibitor *P21<sup>WAF1</sup>* versus pro-apoptotic genes such as *PUMA* (51). A low-intensity response may induce transient cell cycle arrest whereas a higher intensity response could induce apoptosis (66). Where transient cell cycle arrest is induced in response to acute stress, the p53-response is essentially a protect and repair signal (1) and is attenuated once the stress is relieved (63). Because prolonged p53 activation may potentially lead to apoptosis or permanent senescence, the effective attenuation of the p53 response can also be an important determinant of cellular outcome. HDM2 is known to be critical in this attenuation phase (63); the role of HDMX has not previously been determined.

HDM2 is an E3-ligase for itself, as well as p53, and has a short half life in cells; thus changes in its rate of synthesis have an immediate and substantial effect on its cellular abundance. Its P2-promoter contains two p53-responsive elements, as well as other transcription factor-binding sites, which cooperate with p53 to drive a strong transcriptional response upon p53 activation (19,21). Furthermore, the mRNA product of the *HDM2-P2* promoter can be translated into HDM2 more efficiently than that of the constitutive P1 promoter (22). With the use of conditional temperature-sensitive mutants of p53 in murine cells, a p53-induced increase of MDM2 protein abundance was readily detectable, and quickly led to the identification of the p53-responsive promoter (23,67). In contrast, HDMX is a relatively more stable protein in cells (54); it does not in itself possess significant auto-E3 ubiquitin ligase activity. Instead, its rate of turnover is dependent on its

HDM2-dependent ubiquitination. Thus, upon activation of p53 in cells, the increase in HDM2 protein abundance results in increased rates of HDMX degradation. This effect has been demonstrated in experiments using Nutlin-3 (29,59) as the p53-activating agent, although the degradation of HDMX upon Nutlin-3 exposure shows clear cell-type specificity. In addition to this, p53-independent signaling pathways induced by DNA damage, i.e. ATM-dependent phosphorylation of HDMX, further promote its degradation by inhibiting its interaction with the deubiquitinating enzyme, HAUSP (27,68). Thus, in many cells, stresses such as ionizing radiation result in a rapid decrease in HDMX protein levels that, due to relatively low rates of HDMX protein synthesis, remain low for an extended time period. HDMX protein abundance does not, therefore, substantially increase in response to stress and *HDMX* had not been identified as a p53-inducible gene.

We have shown here that *HDMX* does indeed contain a p53-responsive promoter, and that *HDMX* transcription can be induced in response to a wide range of p53-activating signals. The p53-RE in this *HDMX-P2* promoter is a strong match to the defined optimal sequence (51). The fold activation of the *HDMX-P2* promoter by a given amount of p53 is comparable to the *P21<sup>WAF1</sup>* promoter, and greater than that of the *BAX* gene, in which the p53-RE is a weaker match to the consensus. Despite this, the absolute p53-induced activity of the *HDMX-P2* promoter is lower than that of *P21<sup>WAF1</sup>*, and in several cell lines, we found p53 activation does not result in substantial increases in *HDMX-P2* promoter-derived transcripts. Therefore, we conclude that the *HDMX/mdmX-P2* are relatively weak promoters, and may require the activity of factors other than p53 which are not present in some cell types, such as the MRC5 fibroblast line. However, as is the case for *HDM2*, the *HDMX-P2* derived mRNA is substantially more efficiently translated than that derived from the P1 promoter, and does contribute to the abundance of HDMX proteins when it is expressed. Using recombinant vectors encoding synthetic cDNAs corresponding to the *HDMX-P1* and *HDMX-P2* promoter-derived transcripts, we determined that translation of the *HDMX-P2*-derived transcript is initiated from an ATG in exon 1 $\beta$ , giving rise to the HDMX-L form of the protein that has compromised p53-binding and compromised ability to inhibit p53-mediated transcription activation compared to

HDMX. The difference in mobility of the two proteins on SDS-PAGE gels is very slight, and when co-expressed as endogenous proteins it is generally not possible to reliably distinguish between them, thus the presence of HDMX-L within the ~75 kDa band can only readily be determined by the reduced band intensity in cells treated with siRNA targeting the *HDMX-P2* transcript.

P53 activating signals, through both the p53-induced transcription of *HDM2*, as well as post-translational modifications to HDMX itself, generally promote the degradation of HDMX protein. Other specific forms of stress, for example the compound Leptomycin B as we have shown here, can lead to aberrant splicing of HDMX mRNA, or potentially increased degradation as has been shown previously in response to Cisplatin (32) (note that we did not observe this effect of Cisplatin in our analysis of ovarian cancer cell lines, though the concentrations of the drug we used were lower than in the study by Markey *et al* (32)). Thus the net effect of p53-inducible *HDMX* transcription is, depending on the p53-activating agent and the degree of aberrant splicing of the induced transcript, to reduce the extent of DNA damage and ATM-induced reduction in HDMX proteins, and promote the earlier recovery of HDMX protein abundance during the attenuation phase. In the specific case of Nutlin-3, it causes a modest increase in HDMX protein abundance (in cells in which *HDMX-P2* transcripts are not induced Nutlin-3 treatment actually leads to a decrease in HDMX protein abundance). An important general point, therefore, is that whilst the post-translational regulation of HDMX protein preclude a robust increase in its abundance in response to p53 activation, in the absence of its transcriptional induction by p53, its abundance in stressed cells is reduced and the p53 response is enhanced or prolonged, clearly demonstrating the importance of this auto-regulatory feedback mechanism of p53 regulation. The cellular response to ATM-activating DNA damage has been widely studied, and has led to the development of well-defined models of the interplay between the three proteins during different stages of the response, particularly by Wahl and colleagues (7,63). Current data indicate that in proliferating cells HDM2-HDMX heterodimers may be a major form in which HDM2 exists as an active p53 E3-ubiquitin ligase (12,69). In response to ATM-dependent phosphorylation events, both

proteins are rapidly degraded and p53 is consequently activated. HDM2 protein synthesis increases due to p53-dependent transcription of *HDM2*, further reducing HDMX levels and, once the ATM-activating signal dissipates, HDM2 protein abundance increases to high enough levels for homodimers to form, and p53 is thus ubiquitinated and targeted for destruction, attenuating the p53 response. In cells in which *HDMX* transcription is not induced by p53, HDMX protein levels remain low (e.g. supplemental figure S5C); this may be important to allow active HDM2 dimers to effectively bind p53 and promote its ubiquitination, as monomeric HDMX could otherwise compete with HDM2 for p53-binding. Contrasting this, however, in the presence of HDMX, active HDM2 E3 ubiquitin-ligase complexes potentially form at lower concentrations of HDM2. Thus it is of particular interest that, at least in humans, the p53-inducible *HDMX* mRNA encodes a form of HDMX, i.e. HDMX-L, which has reduced p53-binding activity whilst retaining the ability to bind HDM2 and promote its activity. Thus the formation of HDM2-HDMX-L hetero-complexes would expedite the clearance of stress-induced p53 during the attenuation phase, in the absence of competition for p53-binding by HDMX. Precisely how the additional N-terminal 18 amino acids in HDMX-L affects p53 binding remains to be determined, though parallels may exist with the so-called lid region present at the N-terminus of HDM2, which inhibits p53-binding by the p53-binding pocket of this protein (70). The results from our RNAi experiments in ionising radiation- or etoposide-treated breast cancer cells, as compared to MRC5 fibroblasts, are entirely consistent with the above model of HDMX-L function in cells. In the TGCT cell line, N-TERA-2, p53 activation induces a primarily pro-apoptotic response; any role of auto-regulatory feedback loops in these circumstances are less clear, and the cells essentially do not recover from the p53 activating stress. On a final note, it is interesting that, whilst murine *mdmx* does contain a p53-responsive promoter, the p53-inducible transcripts encode MdmX protein, rather than a longer, p53-binding compromised form. The expression of HDMX-L in humans may be a relatively late evolutionary development which engenders further complexity to the p53-response.

Finally, we have in this study performed an in-depth analysis of the role of p53-dependent transcription from the *HDMX-P2* promoter in the cellular response to Nutlin-3. Nutlin-3 is one of the first developed small molecule inhibitors of the p53-HDM2 interaction which bind HDM2 in its p53-binding pocket. HDM2 inhibitors including Nutlin-3 have proven promising anti-cancer agents in pre-clinical cancer models (7,30), and are currently in early phase clinical trials. Whilst Nutlin-3 is able to inhibit the HDMX:p53 interaction to some extent and can inhibit the growth of HDMX-overexpressing cell lines (71), it has also been found that it does not inhibit HDMX as effectively as it does HDM2, and the presence of high levels of HDMX, or the apparent failure of Nutlin-3 to induce the degradation of HDMX can provide relative resistance to Nutlin-3 (29,59,72). Here we have shown that, rather than a failure to degrade HDMX, in the cell lines we have studied Nutlin-3 does not reduce HDMX protein levels largely due to p53-dependent transcriptional activation of *HDMX*, and indeed HDMX protein abundance actually increases somewhat in response to Nutlin-3. RNAi mediated knockdown of the *HDMX-P2* transcript in MCF-7 cells, and other breast cancer cell lines in which this transcript is induced by Nutlin-3, reduces the abundance of HDMX proteins in the Nutlin-3 treated cells. Interestingly, the Nutlin-3 induced increase in p53-protein abundance is also increased in these RNAi-treated cells. Thus, despite the blockade of HDM2-p53 binding in these cells, HDMX is still apparently able to influence p53 degradation. Potentially at the high levels of HDM2 present in Nutlin-3 treated cells, a small proportion of this is still able to bind p53 and target it for ubiquitination or, as has been demonstrated recently, interaction between secondary docking sites in p53 and HDM2 can be sufficient to result in p53 ubiquitination, which can thus occur in the presence of Nutlin-3 (73). In either of these circumstances the presence of HDMX or HDMX-L could potentially promote the ubiquitination of p53 by HDM2 in cells through the formation of heterodimers.

Despite this, we did not detect any substantial effects of pre-treatment with RNAi to *HDMX-P2* on the ability of Nutlin-3 to induce p53-dependent target genes in our experiments in the breast cancer cells, nor was there a marked shift from a cell-cycle arrest to apoptotic response, indeed we only detected effects of

*HDMX-P2* knockdown in MCF-7 cells when the cells were subjected to single cell colony forming assays, conditions whereby a pro-apoptotic response can be favored due to anoikis. One explanation for this general lack of a sensitizing effect is that, in this cell type, the effect of Nutlin-3 is to induce primarily a *p21<sup>WAF1</sup>* response that induces a reversible cell cycle arrest in G<sub>1</sub> phase rather than apoptosis, as has been previously reported (29). It was interesting, therefore, to study the testicular germ cell tumor cells, in which p53 activation induces predominantly a pro-apoptotic response, and in which Li *et al.* (36) have also recently provided some good evidence for the existence of a p53-HDMX auto-regulatory feedback loop.

In these cells Nutlin-3 did not result in a decrease in the abundance of HDMX, in fact, as in MCF-7 cells, there was a small increase. In the N-TERA-2 cell line that we studied, this increase in HDMX was dependent upon the induction of *HDMX-P2* transcripts. Of note, in their analysis which involved the quantification of total *HDMX* mRNA rather than individual promoter-derived transcripts, Li *et al.* did not identify any p53-dependent regulation of HDMX in this particular TGCT cell line; this illustrates the point that, when experiments are performed to specifically identify and manipulate *HDMX-*

*P2* promoter-derived mRNA transcripts, a functional p53-HDMX auto-regulatory feedback loop is demonstrably present in a much wider range of human tumor cells than could be predicted from the analysis and manipulation of total *HDMX* mRNA alone. In N-TERA-2 cells, despite the failure to reduce HDMX, Nutlin-3 still induces a strong apoptotic response. However, it is clear that the upregulation of HDMX expression does limit this Nutlin-3 response, as both the increase in p53 protein abundance, and the expression of p53-responsive proteins, notably PUMA, is upregulated, and both short term survival and long term proliferative potential is reduced when cells are pretreated with RNAi to the *HDMX-P2* transcript. In conclusion, the p53-dependent transcriptional induction of a novel *HDMX* mRNA transcript which is efficiently translated into HDMX-L protein is clearly able to influence the cellular response to p53 activation. A marked difference exists between the apparent ability of cells of different origins to induce *HDMX* expression in response to stress, with likely consequences on the eventual outcome to the cell. These novel findings will help provide further clarity to our increasing understanding of this critical stress-response pathway.

## REFERENCES

1. Vogelstein, B., Lane, D., and Levine, A. J. (2000) *Nature* **408**, 307-310
2. Christophorou, M. A., Ringshausen, I., Finch, A. J., Swigart, L. B., and Evan, G. I. (2006) *Nature* **443**, 214-217
3. Wynford-Thomas, D., and Blaydes, J. (1998) *Carcinogenesis* **19**, 29-36
4. Hupp, T. R., Lane, D. P., and Ball, K. L. (2000) *Biochem J* **352 Pt 1**, 1-17
5. Vassilev, L. T., Vu, B. T., Graves, B., Carvajal, D., Podlaski, F., Filipovic, Z., Kong, N., Kammlott, U., Lukacs, C., Klein, C., Fotouhi, N., and Liu, E. A. (2004) *Science* **303**, 844-848
6. Marine, J. C., and Jochemsen, A. G. (2005) *Biochem Biophys Res Commun* **331**, 750-760
7. Toledo, F., and Wahl, G. M. (2007) *Int J Biochem Cell Biol* **39**, 1476-1482
8. Uesugi, M., and Verdine, G. L. (1999) *Proc Natl Acad Sci U S A* **96**, 14801-14806
9. Shvarts, A., Steegenga, W. T., Riteco, N., Laar, T. V., Dekker, P., Bazuine, M., Ham, R. C. A. V., van Oordt, W. V. D. H., Hateboer, G., van der Eb, A. J., and Jochemsen, A. G. (1996) *EMBO J* **15**, 5349-5357
10. Tang, Y., Zhao, W., Chen, Y., Zhao, Y., and Gu, W. (2008) *Cell* **133**, 612-626
11. Brooks, C. L., and Gu, W. (2006) *Mol Cell* **21**, 307-315

12. Linares, L. K., Hengstermann, A., Ciechanover, A., Muller, S., and Scheffner, M. (2003) *Proc Natl Acad Sci U S A* **100**, 12009-12014
13. Okamoto, K., Taya, Y., and Nakagama, H. (2009) *FEBS Lett* **583**, 2710-2714
14. Uldrijan, S., Pannekoek, W. J., and Vousden, K. H. (2007) *EMBO J* **26**, 102-112
15. Gu, J., Kawai, H., Nie, L., Kitao, H., Wiederschain, D., Jochemsen, A. G., Parant, J., Lozano, G., and Yuan, Z. M. (2002) *J Biol Chem* **277**, 19251-19254
16. Bond, G. L., Hu, W., Bond, E. E., Robins, H., Lutzker, S. G., Arva, N. C., Bargonetti, J., Bartel, F., Taubert, H., Wuerl, P., Onel, K., Yip, L., Hwang, S. J., Strong, L. C., Lozano, G., and Levine, A. J. (2004) *Cell* **119**, 591-602
17. Alt, J. R., Greiner, T. C., Cleveland, J. L., and Eischen, C. M. (2003) *EMBO J* **22**, 1442-1450
18. Onel, K., and Cordon-Cardo, C. (2004) *Mol Cancer Res* **2**, 1-8
19. Zauberman, A., Flusberg, D., Barak, Y., and Oren, M. (1995) *Nucleic Acids Res.* **23**, 2584-2592
20. Danovi, D., Meulmeester, E., Pasini, D., Migliorini, D., Capra, M., Frenk, R., de Graaf, P., Francoz, S., Gasparini, P., Gobbi, A., Helin, K., Pelicci, P. G., Jochemsen, A. G., and Marine, J. C. (2004) *Mol. Cell. Biol.* **24**, 5835-5843
21. Phelps, M., Darley, M., Primrose, J. N., and Blaydes, J. P. (2003) *Cancer Res* **63**, 2616-2623
22. Brown, C. Y., Mize, G. J., Pineda, M., George, D. L., and Morris, D. R. (1999) *Oncogene* **18**, 5631-5637
23. Barak, Y., Gottlieb, E., Juven-Gershon, T., and Oren, M. (1994) *Genes & Dev* **8**, 1739-1749
24. Landers, J. E., Cassel, S. L., and George, D. L. (1997) *Cancer Res.* **57**, 3562-3568
25. Stommel, J. M., and Wahl, G. M. (2004) *EMBO J* **23**, 1547-1556.
26. Chen, L., Gilkes, D. M., Pan, Y., Lane, W. S., and Chen, J. (2005) *EMBO J* **24**, 3411-3422
27. Pereg, Y., Shkedy, D., de Graaf, P., Meulmeester, E., Edelson-Averbukh, M., Salek, M., Biton, S., Teunisse, A. F., Lehmann, W. D., Jochemsen, A. G., and Shiloh, Y. (2005) *Proc Natl Acad Sci U S A* **102**, 5056-5061
28. Wang, Y. V., Leblanc, M., Wade, M., Jochemsen, A. G., and Wahl, G. M. (2009) *Cancer Cell* **16**, 33-43
29. Wade, M., Wong, E. T., Tang, M., Vassilev, L. T., and Wahl, G. M. (2006) *J Biol Chem* **281**, 33036-33044
30. Vassilev, L. T. (2007) *Trends Mol Med* **13**, 23-31
31. Chandler, D. S., Singh, R. K., Caldwell, L. C., Bitler, J. L., and Lozano, G. (2006) *Cancer Res* **66**, 9502-9508
32. Markey, M., and Berberich, S. J. (2008) *Oncogene* **27**, 6657-6666
33. Bouvard, V., Zaitchouk, T., Vacher, M., Duthu, A., Canivet, M., Choisy-Rossi, C., Nieruchalski, M., and May, E. (2000) *Oncogene* **19**, 649-660.
34. Mendrysa, S. M., and Perry, M. E. (2000) *Mol. Cell. Biol.* **20**, 2023-2030
35. Wei, C. L., Wu, Q., Vega, V. B., Chiu, K. P., Ng, P., Zhang, T., Shahab, A., Yong, H. C., Fu, Y., Weng, Z., Liu, J., Zhao, X. D., Chew, J. L., Lee, Y. L., Kuznetsov, V. A., Sung, W. K., Miller, L. D., Lim, B., Liu, E. T., Yu, Q., Ng, H. H., and Ruan, Y. (2006) *Cell* **124**, 207-219
36. Li, B., Cheng, Q., Li, Z., and Chen, J. (2010) *Cell Cycle* **9**, 1411-1420
37. Nakano, K., Balint, E., Ashcroft, M., and Vousden, K. H. (2000) *Oncogene* **19**, 4283-4289
38. De Waard-Siebinga, I., Blom, D. J., Griffioen, M., Schrier, P. I., Hoogendoorn, E., Beverstock, G., Danen, E. H., and Jager, M. J. (1995) *Int J Cancer* **62**, 155-161

39. Tait, L., Dawson, P. J., Wolman, S. R., and Miller, F. R. (1996) *Int. J. Onc.* **9**, 263-267
40. Blaydes, J. P., and Hupp, T. R. (1998) *Oncogene* **17**, 1045-1052
41. Chen, J., Marechal, V., and Levine, A. J. (1993) *Mol. Cell. Biol.* **13**, 4107-4114
42. Kessler, B. M., Fortunati, E., Melis, M., Pals, C. E., Clevers, H., and Maurice, M. M. (2007) *J Proteome Res* **6**, 4163-4172
43. Wiederschain, D., Gu, J., and Yuan, Z. M. (2001) *J Biol Chem* **276**, 27999-28005
44. Cullen, B. R. (2006) *Nat Methods* **3**, 677-681
45. Lam, S., Lodder, K., Teunisse, A. F., Rabelink, M. J., Schutte, M., and Jochemsen, A. G. (2010) *Oncogene* **29**, 2415-2426
46. Brummelkamp, T. R., Bernards, R., and Agami, R. (2002) *Science* **296**, 550-553
47. Dirac, A. M., and Bernards, R. (2003) *J Biol Chem* **278**, 11731-11734
48. Xirodimas, D., Saville, M. K., Edling, C., Lane, D. P., and Lain, S. (2001) *Oncogene* **20**, 4972-4983
49. Ohkubo, S., Tanaka, T., Taya, Y., Kitazato, K., and Prives, C. (2006) *J Biol Chem* **281**, 16943-16950
50. Shvarts, A., Bazuine, M., Dekker, P., Ramos, Y. F., Steegenga, W. T., Merckx, G., van Ham, R. C., van der Houven van Oordt, W., van der Eb, A. J., and Jochemsen, A. G. (1997) *Genomics* **43**, 34-42
51. Inga, A., Storici, F., Darden, T. A., and Resnick, M. A. (2002) *Mol. Cell. Biol.* **22**, 8612-8625
52. Rallapalli, R., Strachan, G., Cho, B., Mercer, W. E., and Hall, D. J. (1999) *J Biol Chem* **274**, 8299-8308
53. Pan, Y., and Chen, J. (2003) *Mol. Cell. Biol.* **23**, 5113-5121
54. Kawai, H., Wiederschain, D., Kitao, H., Stuart, J., Tsai, K. K., and Yuan, Z. M. (2003) *J Biol Chem* **278**, 45946-45953
55. Stott, F. J., Bates, S., James, M. C., McConnell, B. B., Starborg, M., Brookes, S., Palmero, I., Ryan, K., Hara, E., Vousden, K. H., and Peters, G. (1998) *EMBO J.* **17**, 5001-5014
56. LeBron, C., Chen, L., Gilkes, D. M., and Chen, J. (2006) *EMBO J* **25**, 1196-1206
57. Burger, H., Nooter, K., Boersma, A. W., van Wingerden, K. E., Looijenga, L. H., Jochemsen, A. G., and Stoter, G. (1999) *Int J Cancer* **81**, 620-628
58. Bauer, S., Muhlenberg, T., Leahy, M., Hoicyk, M., Gauler, T., Schuler, M., and Looijenga, L. (2010) *Eur Urol* **57**, 679-687
59. Patton, J. T., Mayo, L. D., Singhi, A. D., Gudkov, A. V., Stark, G. R., and Jackson, M. W. (2006) *Cancer Res* **66**, 3169-3176
60. Hu, W., Feng, Z., Teresky, A. K., and Levine, A. J. (2007) *Nature* **450**, 721-724
61. Vousden, K. H., and Ryan, K. M. (2009) *Nat Rev Cancer* **9**, 691-700
62. Blaydes, J. P., and Wynford-Thomas, D. (1998) *Oncogene* **16**, 3317-3322
63. Wahl, G. M. (2006) *Cell Death Differ* **13**, 973-983
64. Gilkes, D. M., Chen, L., and Chen, J. (2006) *EMBO J* **25**, 5614-5625
65. Wang, Y. V., Wade, M., and Wahl, G. M. (2009) *Cell Cycle* **8**, 3443-3444
66. Knights, C. D., Catania, J., Di Giovanni, S., Muratoglu, S., Perez, R., Swartzbeck, A., Quong, A. A., Zhang, X., Beerman, T., Pestell, R. G., and Avantaggiati, M. L. (2006) *J Cell Biol* **173**, 533-544
67. Wu, X., Bayle, J. H., Olson, D., and Levine, A. J. (1993) *Genes & Dev* **7**, 1126-1132
68. Meulmeester, E., Maurice, M. M., Boutell, C., Teunisse, A. F., Ovaa, H., Abraham, T. E., Dirks, R. W., and Jochemsen, A. G. (2005) *Mol Cell* **18**, 565-576
69. Kawai, H., Lopez-Pajares, V., Kim, M. M., Wiederschain, D., and Yuan, Z. M. (2007) *Cancer Res* **67**, 6026-6030

70. McCoy, M. A., Gesell, J. J., Senior, M. M., and Wyss, D. F. (2003) *Proc Natl Acad Sci U S A* **100**, 1645-1648
71. Laurie, N. A., Donovan, S. L., Shih, C. S., Zhang, J., Mills, N., Fuller, C., Teunisse, A., Lam, S., Ramos, Y., Mohan, A., Johnson, D., Wilson, M., Rodriguez-Galindo, C., Quarto, M., Francoz, S., Mendrysa, S. M., Guy, R. K., Marine, J. C., Jochemsen, A. G., and Dyer, M. A. (2006) *Nature* **444**, 61-66
72. Hu, B., Gilkes, D. M., Farooqi, B., Sebti, S. M., and Chen, J. (2006) *J Biol Chem* **281**, 33030-33035
73. Wallace, M., Worrall, E., Pettersson, S., Hupp, T. R., and Ball, K. L. (2006) *Mol Cell* **23**, 251-263

### ACKNOWLEDGMENTS

We are grateful to Phil Coates for providing cDNAs from irradiated mouse tissues, Gigi Lozano for making available the *p53/mdm2* double knockout MEFs, Gordon Peters for the gift of NARF cells and anti-p14ARF antibody 4C6 and Karen Vousden for the gift of the p53-inducible SAOS-2 cells. We thank Theo van Laar for the irradiation of MEFs and Ute Rolle for excellent technical assistance.

### FOOTNOTES

\*This work was funded by a project grants from the Association for International Cancer Research to JPB (#07-0437) and to AGJ (#05-273; by Dutch Cancer Society Grant UL 2006-3595, and by EC FP6 funding (contract 503576) to AG Jochemsen. This publication reflects the authors' views and not necessarily those of the European Community. The EC is not liable for any use that may be made of the information contained. Furthermore, part of this work was supported by the Wilhelm-Sander-Stiftung (2006.010.1), Deutsche Krebshilfe (grant 108424), the Wilhelm-Roux-Programm of the University of Halle-Wittenberg (grant 12/40), and the Fritz-Thyssen-Stiftung (Az 10.09.2.117).

The costs of publication of this article were defrayed in part by the payment of page charges. This article must therefore be hereby marked “*advertisement*” in accordance with 18 U.S.C. Section 1734 solely to indicate this fact.

<sup>1</sup>The abbreviations used are: IPs, immunoprecipitation; MEFs, murine embryo fibroblasts; p53-RE, p53-response element; TGCT; testicular germ cell tumor; NCS, Neocarzinostatin; LMB, Leptomycin B; Act.D, Actinomycin D.

### FIGURE LEGENDS

**Figure 1. A novel promoter in intron 1 of *HDMX* contains a functional p53 binding site.** A, Map of 5' end of *HDMX* gene, showing the position of the novel exon 1 $\beta$  as defined by EST DB137351. A potential p53-binding site in intron 1 is compared to the consensus p53-binding sequence. Inverted triangles show the known translation start site in exon 2, and an in-frame ATG in exon 1 $\beta$ , initiation of translation from which would incorporate 18 additional amino acids at the N-terminus of *HDMX* (MQNLSKVLPTDCSFFTTK). B, MCF-7 cells were transfected with 25 nM control (solid bars) or p53 siRNA (open bars), followed 24 h later by transfection with pGL3basic, HDMXP2luc01 or p21-luc reporter plasmids. Reporter activity was assayed after a further 48 h. (n=6). Western blotting demonstrates efficacy of the siRNA. C, (i) MCF-7 cells were transfected

with the HDMXP2luc deletion constructs shown. Numbering is relative to start of exon 2. (n $\geq$ 9). (ii) H1299 cells were transfected with the HDMXP2luc deletion constructs plus 25 ng pc53SN3 (black bars) or empty vector control (white bars). (n=5). D, MCF-7 cells were transfected with HDMXP2luc01 (solid bars) or HDMXP2luc01 $\Delta$ p53RE (open bars) along with increasing amounts of dominant negative p53 fragment (DDp53). (n=6). E, MCF-7 cells were transfected with the stated reporter plasmid. Following removal of transfection mix after 4 h, cells were exposed to media only (Black bars), 200  $\mu$ M 5-fluorouracil (gray bars) or 5  $\mu$ M Nutlin-3 (white bars) for 24 h before luciferase activity was determined. (n=6).

**Figure 2. The endogenous *HDMX-P2* promoter is induced by p53.** A, SAOS-2 cells containing a doxycycline-inducible p53 construct and control SAOS-2 cells were treated with doxycycline for 24 h, after which cells were harvested for protein analysis, mRNA analysis and chromatin-immunoprecipitation (ChIP). RT-PCR and Western blotting was used to determine expression of mRNAs and proteins. Changes in recruitment of p53 to the p53REs in *HDMX-P2*, *HDM2-P2* and *p21<sup>WAF1</sup>* promoters are indicated as fold-increase in recovery of that specific chromatin fragment. B, MCF-7 cells were treated with Nutlin-3 (5  $\mu$ M) for the indicated times, while MPE600, ZR75-30 and SAOS-2 cells were treated either with Nutlin-3 (10  $\mu$ M; 6 h) or Etoposide (20  $\mu$ M; 6 h) prior to harvest and analysis by Western blotting and RT-PCR. C, Stable derivatives of 92.1 cells expressing either control shRNA or p53-shRNA were treated with Nutlin-3 (10  $\mu$ M; 24 h), after which RNA was extracted and expression of *HDMX-P2* and *p21<sup>WAF1</sup>* determined by real-time PCR. MCF-7 cells were transfected with control or p53 siRNA. 48 h later the cells were exposed to 5  $\mu$ M Nutlin-3 prior to analysis of mRNA expression by RT-PCR. D, VH10hTERT and MPE600 cells were treated with Nutlin-3 (10  $\mu$ M) for indicated periods, after which cells were harvested and processed for analysis of mRNA expression and protein expression by RT-PCR and Western blotting. In addition, ChIP was used to determine the recruitment of p53 to the p53REs in the *HDMX-P2*, *HDM2P2* and *p21<sup>WAF1</sup>* promoters. E, NARF cells (U2OS cells containing IPTG-inducible p14ARF construct) were treated with IPTG or mock-treated for indicated time periods. Cells were harvested and RT-PCR and Western blotting was used to determine expression of indicated mRNAs and proteins. p14<sup>ARF</sup> expression was investigated by immunofluorescence (supplemental figure S2C). F, OAW-42 ovarian cancer cells that express wild-type p53 were exposed to 10  $\mu$ M Cisplatin for the indicated times before being prepared for analysis by RT-qPCR. *HDMX-P2* induction by Cisplatin in other cell lines with varying p53 status is shown in supplemental figure S2D.

**Figure 3. The p53-responsive promoter is conserved in the mouse *Mdmx* gene.** A, Schematic representation of the 5' end of the *Mdmx* gene showing the location of the *Mdmx* exon 1 $\beta$  and the p53RE in relation to exon 1 and exon 2. B, Mouse embryo fibroblasts were transduced with lentiviruses expressing control shRNA or p53-shRNA. Three days later, cells were seeded and next day treated with Nutlin-3 (10  $\mu$ M) for 2 and 7 h, or mock-treated. Cells were harvested and expression of indicated proteins and mRNAs was determined by Western blotting and RT-PCR. C, B16F10 mouse melanoma cells expressing wild-type p53 or p53-null MEFs were treated with Nutlin-3 (10  $\mu$ M, 6 h). Subsequently, cells were harvested and processed for analysis by RT-PCR, Western blotting and Chromatin-Immunoprecipitation (ChIP). D, cDNAs made from RNAs extracted from the bone marrow of C57/BL6 mice at the indicated time points after exposure to 4 Gy ionizing radiation were provided by Dr. Philip Coates, University of Dundee, UK, and were analyzed by RT-PCR.

**Figure 4. mRNA transcribed from the *HDMX P2* promoter is efficiently translated into a long form of HDMX protein.** A, RNA transcribed from the indicated plasmids were translated *in vitro* using the rabbit reticulocyte lysate system. HDMX expression was determined by Western blotting. Upper panel, short exposure; lower panel, long exposure. B, H1299 cells in 6-well plates were transfected with 85 ng pEGFP-N1, 0.33  $\mu$ g pc53SN3 and 0.67  $\mu$ g pHis6Ub. 1.33  $\mu$ g HDMX plasmid and 0.67  $\mu$ g or 2  $\mu$ g (3x) pHDM2 were also added where stated. 24 h post-transfection cells were lysed and His-tagged proteins purified using Ni<sup>2+</sup>-NTA agarose beads. HDM2, HDMX, p53 and GFP expression were determined by Western blotting. C, MCF-7 cells were transfected with the indicated constructs (HDMX-P1 and HDMX-P2, 100 ng, 200 ng, and 400 ng; Flag-p53, 200 ng). Next day,

cells were harvested and protein extracts were used for immunoprecipitation with anti-HA or anti-Flag antibodies, and a non-specific control. Immunoprecipitated proteins and total cell extracts were analyzed by Western blotting. D, 174-2 *p53/mdm2* double-knockout mouse embryonic fibroblasts were transfected with p21-luc along with 300 pg pc53SN3 (open bars) or empty vector control (solid bars) and 50, 100 or 200 ng of the indicated HDMX expression plasmid 48 h before luciferase activity was determined. Data are pooled from three independent experiments (n=9). Expression of the ectopically expressed proteins is shown in supplemental figure S4E. E, MCF-7 cells stably transfected with either HDMX- or HDMX-L expression vector, or empty vector were treated with Nutlin-3 (10  $\mu$ M) for 6 h. Cells were harvested, RNA extracted and expression of indicated mRNAs determined by real-time RT-PCR. F, Left panel: MCF-7 cells stably transfected with either HDMX- or HDMX-L expression vector, or empty vector were seeded into 96-well plates (1000 cells/well), each cell line in 12 wells (left panel) or 9 wells (right panel). Next day cells were incubated in triplicate with indicated concentrations Nutlin-3 or Actinomycin D. Relative survival of treated cells compared to mock-treatment was determined after 72 hrs of incubation by WST-1 assay. Experiment was repeated at least twice with similar results. Shown is a representative experiment. G, MCF-7 cells stably transfected with either HDMX- or HDMX-L expression vector or empty vector were seeded into 6-well plates (10,000 cells/well). Next day the cells were treated with indicated concentrations of Nutlin-3 for 48 h, or with Actinomycin D (1.0 nM) for 8 or 48 h. All conditions in duplicate. After the treatments, medium was replaced with fresh growth medium and cells were allowed to grow. All cells were fixed 10 days after seeding, and stained with Giemsa. Plates were scanned on Odyssey Imaging system, LI-COR Biosciences (examples shown in lower panels), relative number of cells quantified, and relative survival compared to mock-treated controls is shown in the upper panels. Experiment was repeated at least twice with similar results.

**Figure 5. The role of p53-dependent transcription of *HDMX-P2* in the cellular response to DNA damage.** A, 48 h after transfection with the indicated siRNAs MCF-7 cells were exposed to 5 Gy ionizing radiation. Cell pellets for analysis were prepared at the indicated time points post-irradiation. Quantification shows the abundance of the indicated proteins mean  $\pm$ SEM of seven independent experiments. HDM2 and p21<sup>WAF1</sup> are shown in supplemental figure S5B. Open bars, control siRNA; solid bars, *HDMX-P2* siRNA. B, MCF-7 and MPE600 infected with lentivirus encoding either control or *HDMX-P2* shRNA were exposed to 20  $\mu$ M Etoposide (E) or 10  $\mu$ M Nutlin-3 (N) for 2 h, or mock-treated. Drugs were then washed away and the cells cultured in fresh medium until lysed for analysis. Expression of *HDMX* mRNAs was determined 8 h after addition of the drugs or mock-treatment. The blots show the changes in protein expression upon Etoposide treatment. Times shown in protein analyses are from the addition of drug. C, N-TERA-2 cells transduced with lentivirus encoding either control- or *HDMX-P2* shRNA were exposed to 10  $\mu$ M Nutlin-3 (N) or Etoposide (20  $\mu$ M) for 2 hours, after which the drug was washed away and the cells cultured in fresh medium until harvested for analysis. *HDMX* mRNA expression was determined 8 h after addition of the drugs and after mock-treatment. Western analysis shows the changes in protein expression upon Etoposide treatment.

**Figure 6. Role of p53-dependent transcription of *HDMX-P2* in the cellular response to Nutlin-3.** A, MCF-7 cells were transfected with siRNA to HDMX exon 1 $\beta$  (*HDMXP2*), ctr1 and ctr2 siRNAs which differ from *HDMXP2* siRNA by 4 bases in the seed and central regions respectively, and control siRNA. 48 h later cells were exposed to 0 or 5  $\mu$ M Nutlin-3 for 6 h. RT-PCR and Western blots show results from a representative of three independent experiments. Quantification show mean $\pm$ SEM changes in protein abundance for the three experiments. HDM2 and p21<sup>WAF1</sup> data are shown in supplemental figure S6A. Open bars, 0  $\mu$ M Nutlin-3; solid bars, 5  $\mu$ M Nutlin-3. B, MCF-7 and MPE600 infected with lentivirus encoding either control or *HDMX-P2* shRNA were treated with Nutlin-3 as described in Fig. 5B. The blots show the changes in protein expression upon Nutlin-3 treatment. Times shown in protein analyses are from the addition of drug. PCR analysis of mRNA transcripts following exposure of these cells to Nutlin-3 is shown in Fig. 5B. C, MCF-7 cells were transfected with the indicated siRNAs; 48 h later cells were reseeded into 6-well plates (100 cells/plate). After 24 h cells were exposed to solvent control (open bars) or 5  $\mu$ M Nutlin-3 (solid bars) for 24 h. Colonies were counted after a further 11 days (n=3). The effect of Nutlin-3 on the

percentage of colonies in the presence of each siRNA is shown. D, N-TERA-2 cells transduced with lentivirus encoding either control- or *HDMX-P2* shRNA were exposed to Nutlin-3 (10  $\mu$ M) as described in Figure 5C. *HDMX* mRNA expression was determined 8 h after addition of the drug and after mock-treatment, and is shown in Figure 5C. Western analysis shows the changes in protein expression upon Nutlin-3 treatment. Times shown in protein analyses are from the addition of drug, which was removed after 2 h. E, N-TERA-2 cells expressing the indicated shRNAs were seeded into 6-well plates (10,000 cells/well). Next day, cells were mock-treated or treated with Nutlin-3 (2  $\mu$ M, 4  $\mu$ M), for 24 h; all in duplicate. Medium was replaced by fresh growth medium lacking Nutlin-3, and cells were cultured for additional 6 days. Cells were fixed, and relative survival determined as mentioned by Figure 4G. F, N-TERA-2 cells expressing the indicated shRNAs were seeded into 96-well plates (1,000 cells/well; each cell line in 9 wells total). Next day, Nutlin-3 was added (0, 2 or 4  $\mu$ M), and cells were cultured for additional 72 hrs. Relative survival of treated cells was determined with the use of WST-1 assay. Data shown are the averages of three independent experiments.

# Figure 1

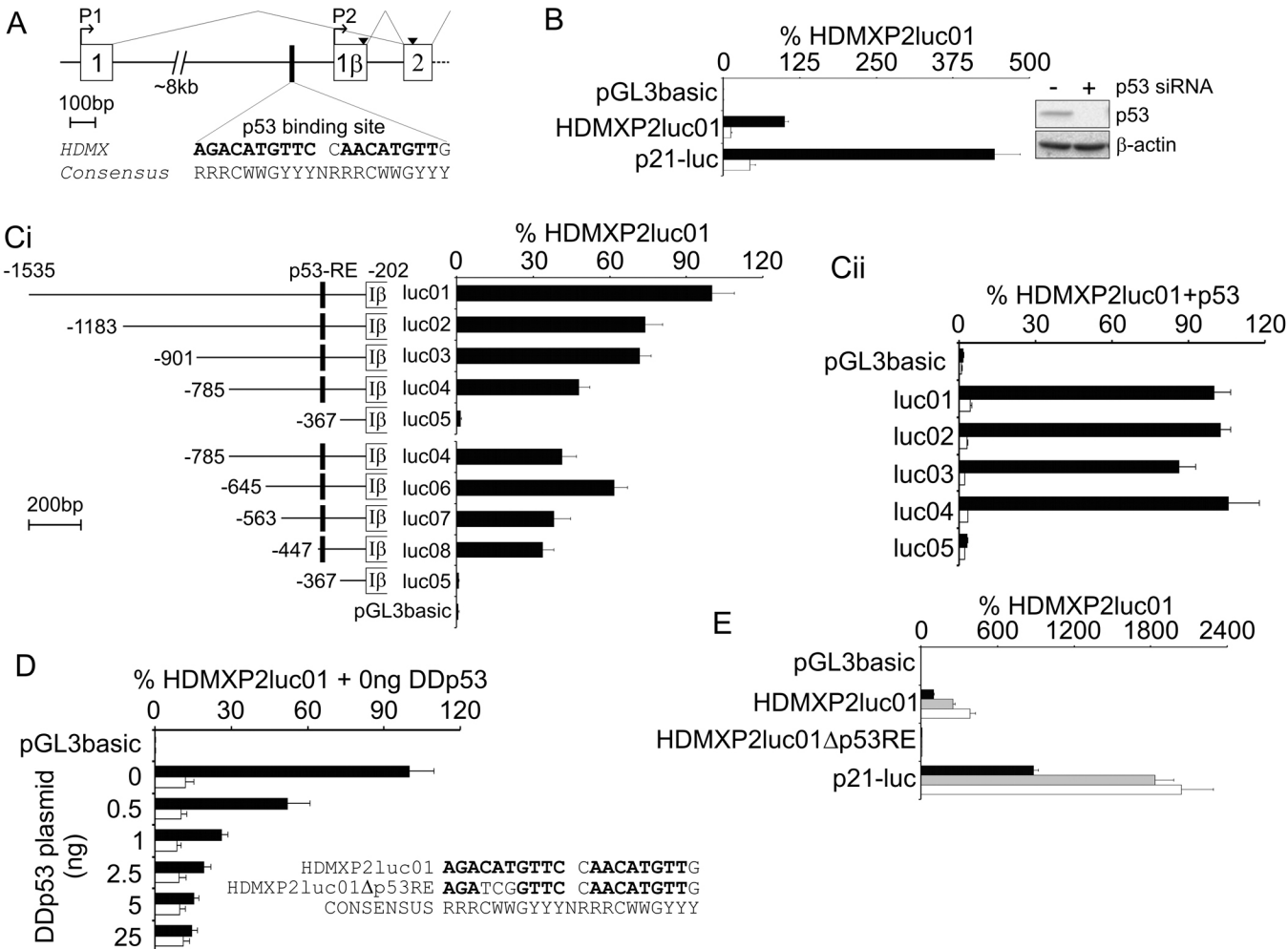


# Figure 2

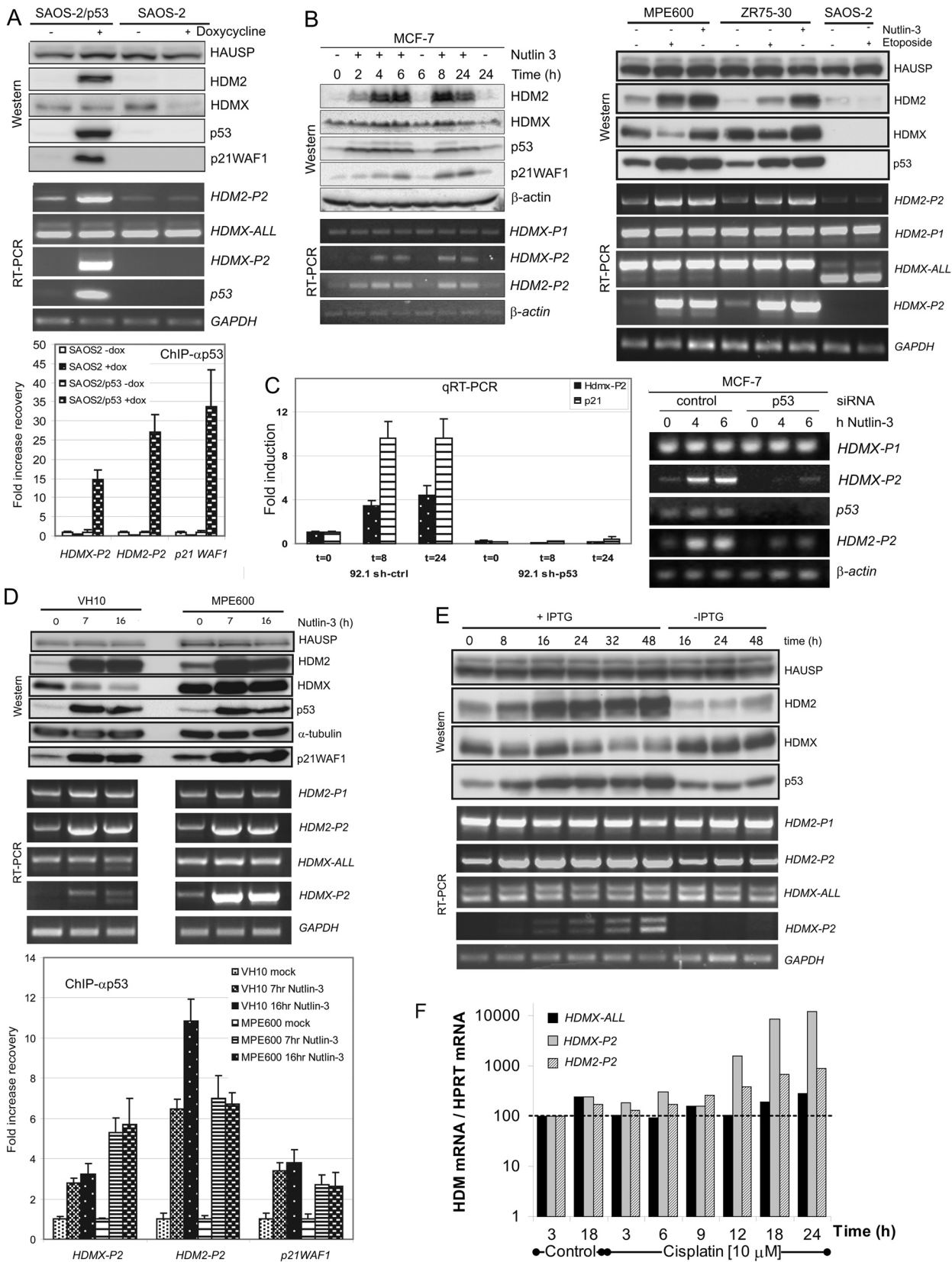


# Figure 3

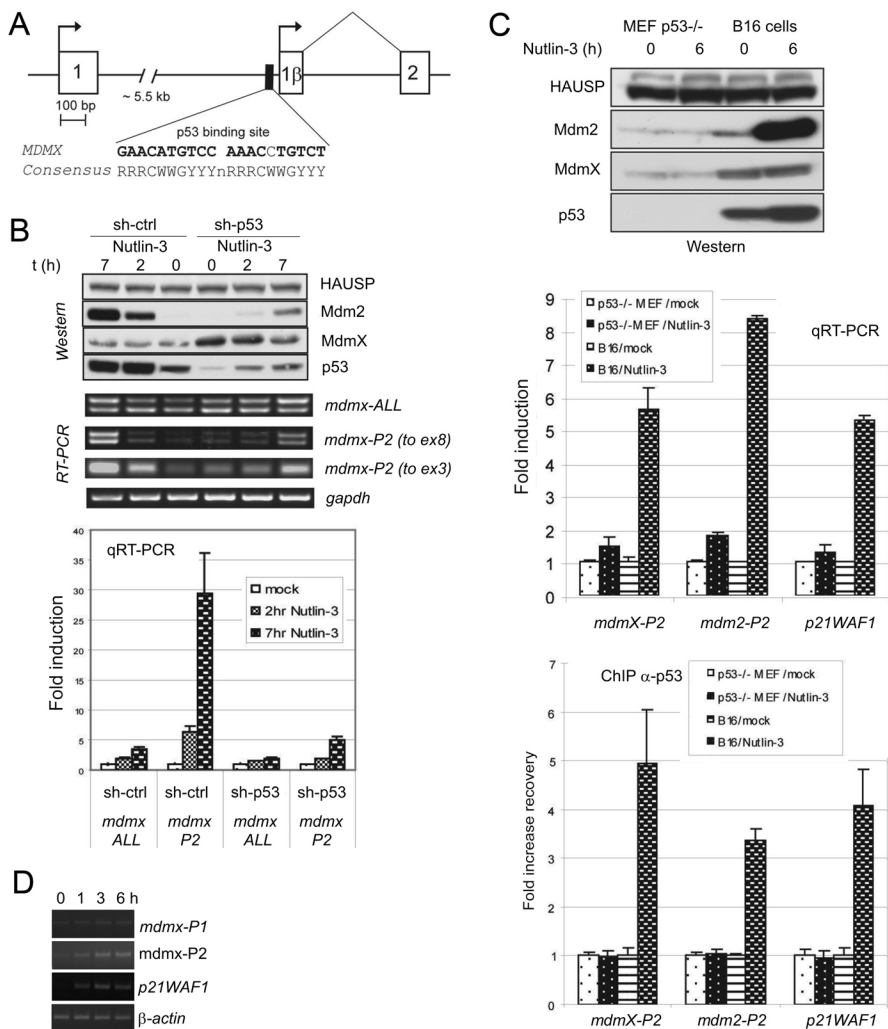


# Figure 4

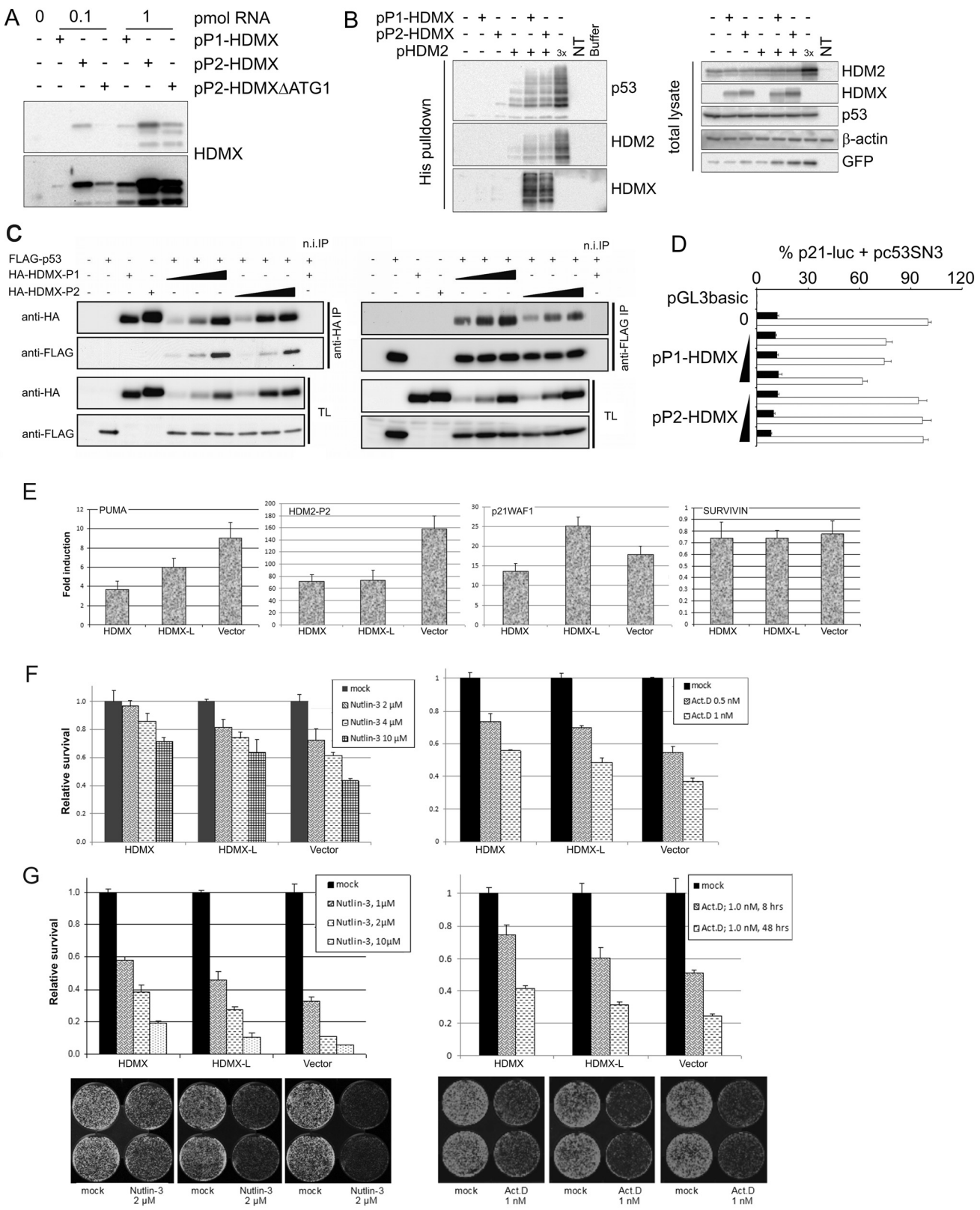
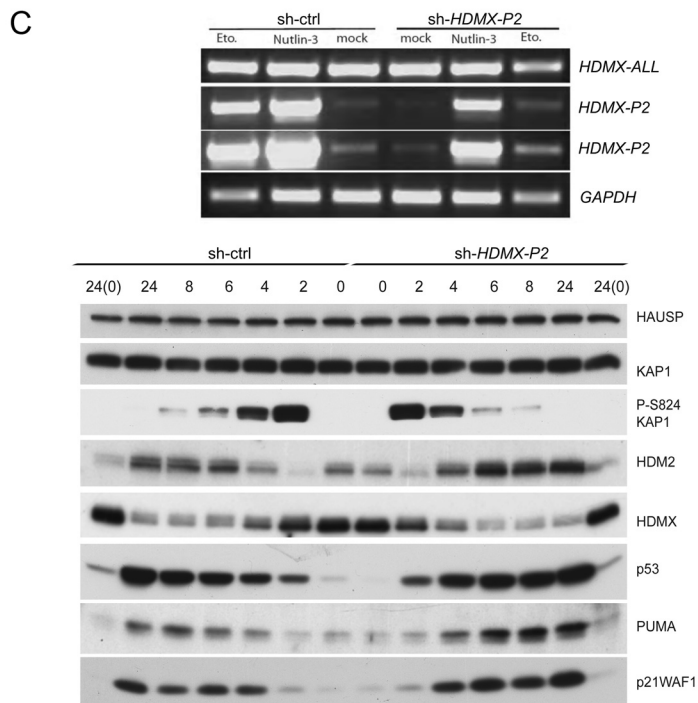
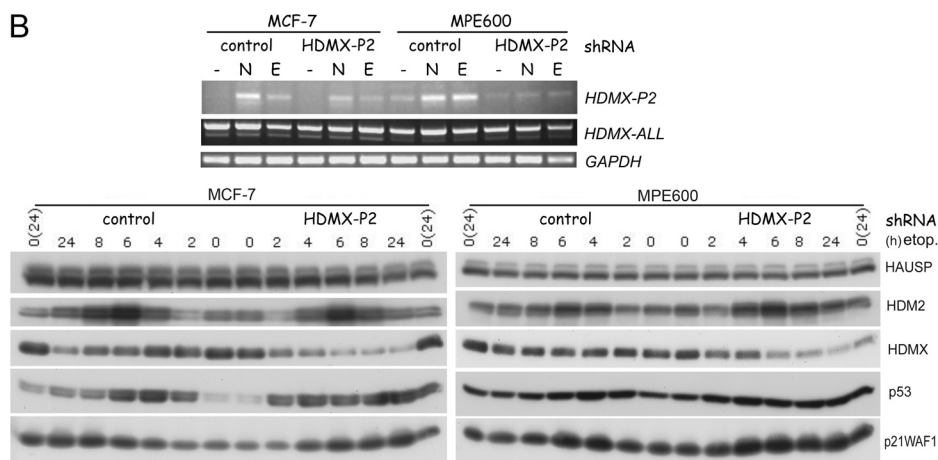
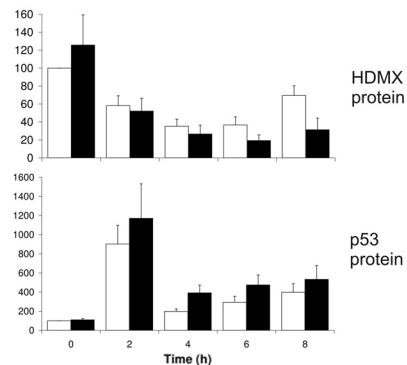
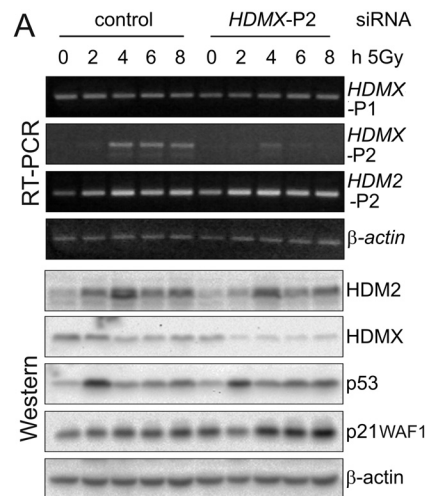


Figure 5



**Figure 6**

